UTS UNIVERSITY OF TECHNOLOGY SYDNEY

Finite Element Analysis of Cracked Concrete Structures Due to Alkali-Silica Reaction

by Mohitkumar Chaudhary

Thesis submitted in fulfilment of the requirements for the degree of

Master of Engineering (Research)

under the supervision of

Dr Mina Mortazavi and A/ Prof. Sanjay Nimbalkar, UTS

University of Technology Sydney
Faculty of Engineering and Information Technology

April 2024

Certificate of Original Authorship

I, ***Mohitkumar Chaudhary***, declare that this thesis is submitted in fulfilment of the requirements for the award of ***Master of Engineering (Research)***, in the *School of Civil and Environmental Engineering, Faculty of Engineering and Information Technology* at the University of Technology Sydney.

This thesis is wholly my own work unless otherwise referenced or acknowledged. In addition, I certify that all information sources and literature used are indicated in the thesis.

This document has not been submitted for qualifications at any other academic institution.

This research is supported by the Australian Government Research Training Program.

Signature: Production Note:
Signature removed prior to publication.

Date: 29.04.24

Acknowledgements

I owe a great deal of gratitude to the several people who have generously supported me over the past couple of years in various ways in order for me to finish this thesis.

I want to start by sincerely thanking my principal supervisor, Dr. Mina Mortazavi, for allowing me to work on this exciting research and for providing me with outstanding supervision and support throughout my time as a student at UTS. I owe her a sincere debt of gratitude for letting me freely examine the research while also making recommendations. I also want to express my gratitude to my co-supervisor, Associate Professor Sanjay Nimbalkar, for contributing his invaluable experience and knowledge in a number of thought-provoking conversations that went above and beyond the parameters of my master's thesis.

My greatest appreciation goes out to Dr Nadarajah Gowripalan for being a wonderful mentor and providing me with an excellent research idea. I am appreciative to have had him as a role model who consistently demonstrated kindness and support for his pupils and colleagues.

Finally, I would like to thank Australian Government and the Australian Government Research Training Program, for granting funds for this research.

List of Publications

Conference:

M. Chaudhary, M. Mortazavi, S. Nimbalkar, 2022. *Finite element modelling of cracked concrete structures affected by Alkali-Silica Reaction.* Proceedings of the IASTEM – 1356th International Conference on Civil and Architectural Engineering (ICCAE), Sydney, Australia, pp. 1-5.

This Conference paper received Best & Excellent paper award.

Journal:

M. Chaudhary, M. Mortazavi, S. Nimbalkar, 2022. "Finite Element Modelling of Cracked Concrete Structures affected by Alkali-Silica Reaction"*, International Journal of Advances in Mechanical and Civil Engineering (IJAMCE) ,* pp. 1-5, Volume-9, Issue-5.

Table of Contents

List of Figures

List of Tables

Abstract

Alkali-Silica reaction in concrete, often referred to as concrete cancer, is a problem causing significant loss in the structural integrity of concrete structures. This chemical reaction produces a gel-like by-product that expands and forms pressure, leading to crack formation. This process decreases the mechanical properties of concrete, reducing its lifespan and affecting its durability and strength. It is considered a dangerous distress mechanism affecting global concrete infrastructure.

ASR can be minimized by using supplemental cementitious materials or non-reactive aggregates. Diagnosing ASR for existing structures and minimizing restoration costs is crucial. However, proper techniques are needed to quantify damage and know the capacity of ASR-affected concrete members. This helps structural engineers develop macro models and compute flexural capacity, enabling effective management and restoration solutions for infrastructure.

Many approaches have been employed to thoroughly understand the ASR mechanism and expansion. However, to this date, the ASR mechanism remains limitedly understood. Practicing engineers need a knowledge base to check and analyse an ASR affected beam. A modelling method is required such that engineers can consider ASR effects in designing a beam. For this understanding, an important question needs to be addressed: **How can material properties be used to introduce ASR effects in a concrete beam model? And how to develop a modelling technique using material properties to assess the Ultimate Flexural capacity of the ASR-affected beam.** To understand the influence of ASR reaction on the strength capacity of concrete members, it is important to develop a model to obtain ASR effects and the extent of strength reduction.

The importance and the need for research in modelling ASR-affected concrete beam are evident. To overcome this problem, a modelling technique is developed, and macro-scale beam models are prepared using finite element software. By defining the material properties, ASR effects are introduced & the degradation in the strength is investigated. Using the Australian Code for Concrete Structures

AS3600, the beam models are designed, and flexural capacity is checked. The results obtained from the model are then compared to the experimental data. This research builds a modelling technique for a beam model that shows how the Alkali-Silica Reaction effects are introduced and how the model helps assessing the flexural capacity of an ASR affected concrete beam.

CHAPTER 1: INTRODUCTION

1.1. Background

The alkali-silica reaction (ASR), called concrete cancer, is considered one of the most severe long-term causes of durability loss in concrete structures. The reaction has various factors contributing to its beginning and growth. The concrete infrastructure suffering from ASR must undergo reconstruction and maintenance costs worldwide. The development of the reaction occurs with the growth of an expansive gel that causes micro-structural cracks, which can eventually lead to macro-cracks and, thus, the degradation of concrete.

Alkali-Silica Reaction can cause far more damage to the structure due to the degradation of not only concrete but also its mechanical properties. The rupture of the structure's structural integrity is caused by loss of mechanical properties or strength.

Swamy and Al-Asali (1988) illustrated that Alkali Silica Reaction (ASR) drastically reduces the strength of concrete. Multon et al. (2004) showed that the reduction in strength causes cracks to form; the modulus of elasticity is also highly affected. It induces excessive swelling that results in significant deformations that exceed the expansion of concrete brought on by ASR-generated forces that weaken and cause damage to the substance. So, whenever feasible, avoid ASR by choosing non-reactive aggregates. If using reactive aggregates is unavoidable, it is necessary to put into practice measures like limiting the total alkali in the concrete mixture and using additional cementitious ingredients. Structures that are already experiencing ASR, however, need to be evaluated. As a result, precise methods are required to assess ASR impacts on concrete strength. For rehabilitation objectives, instruments are necessary to record the observed behavior and foresee consequences and potential failure in the long term.

1.2. Research Aims and Objectives

The causes of ASR effects in concrete members are discussed in this research study, as well as their advancement. This study focuses on how the mechanical properties of concrete are lost due to ASR and how this loss affects concrete's flexural strength. The theory of model development and the modelling of concrete members utilizing a *novel* method for simulating ASR-affected structures are two important investigations of this research. The novel method is based on modelling concrete structures, such as a beam, with layers within the section of the beam. The layers having different & reduced strength values represent the loss of strength in ASR phenomena, which causes expansion & cracking. The results and comparisons with prior research are offered to support the models' validity. The main objective of this study is the development of the model and its utility for assessing the flexural strength of concrete.

In order to achieve this major goal, the following significant objectives are developed:

1. Propose a novel modelling method for ASR-affected structures that are related to the theories and findings of current research. Throughout the years, models have been developed that can depict the strength and loss in capacities of an ASR-affected beam. However, the need for developing a modelling technique remains to incorporate the modelling technique into the design of beams based on a concrete code; in this research, Australian Concrete Code AS3600. The novel modelling technique is based on material properties and not pre-defined stress or strain field data; no pre-defined expansion data; it is based on creating geometry by dividing the beam into layers and inputting reduced strength properties for each layer that implies the ASR effects at structural integrity level. Moreover, the model can also be used for manual computation of flexural strength. Such suitability and availability of using the model in both; software and manual computation makes this modelling method *novel*.

2. Create a numerical model reflecting the loss in mechanical properties and impacts of ASR based on a novel approach and experimental research. The model

can depict the effects of loss in properties based on the varying moduli and varying strength properties. The moduli data is the input that represents the loss in strength. The model responds to the decreasing properties, and using the outcome, the deterioration rate and the results are discussed. The data used for modelling is extracted from the literature. Models are created in ABAQUS using the ASR-reduced strength properties from the literature. Material properties are selected from experimental studies and for creating the Models, boundary conditions are used as per the actual experimental setup. The assumptions are made for choosing the thickness of layers and it is based on the literature review in Chapter 2 & 3.

3. Using the outcomes of the experiments to validate the numerical models. The moduli data is the input that represents the loss in strength. For validation, experiments with beam model are chosen where the comparison is made between the normal beam and ASR affected beam. These beams are recreated in ABAQUS using modelling technique. The numerical models respond to the ASR reduced properties and using the outcome, the load vs displacement curves of the numerical models are compared to the load-displacement curves of existing experimental results. So, the recreation of the experimented beams and comparison with the same, completes the validation step of layered modelling technique This way the numerical model is validated based on the

existing research.

4. Determine the loss in flexural strength based on the loss of mechanical attributes assumed in the model concept and included into the numerical model. The idea of inputting the decreasing mechanical properties in the numerical model represents the special theory of stress block for a rectangular beam cross section for the ASR affected concrete. The loss in elastic modulus affects the concrete compressive strength because of linear proportional relationship. The 4 layers of the ASR beam section will have different compressive strength. This information is used to find the loss in the compressive strength and also, to find the loss in ultimate flexural strength of the beam section. This method is the validated using numerical model and is used to compute the loss in strength in affected and non-

affected beams. It is shown that the experimental results match with numerical model's computed losses in strength.

1.3. Research Gaps

It is necessary to have a better understanding of ASR impacts in relation to crack formation and capacity evaluation of concrete structures affected by ASR, and this can be done by addressing a number of research questions based on the literature review on the important topics. The following are the questions:

Important issues relating to the loss in the mechanical properties of concrete brought on by ASR are covered in the literature review in **Chapter 2**, such as questions: (i) What factors contribute to concrete's loss of elasticity when exposed to ASR? (ii) How does ASR affect the elasticity modulus? **Chapter 3** discusses (i) how ASR-induced cracking causes the differential expansion and deterioration of a beam cross-section. and (ii) How can the ASR-induced cracking mechanism be modelled into a layered beam model? The factors impacting concrete's strength are covered in this chapter. Based on the reviews of many researchers, a layered model is developed that suggests that the degradation of the concrete domain is in layers of cracks. This model philosophy is developed based on current research findings.

In **Chapter 4**, the impacts of ASR on the structural capacity of reinforced concrete structures and the modelling technique are addressed. How can the fluctuating moduli be processed as data in the modelling program? How does the modelling technique reflect strength loss, and how the strength loss for ASR-affected structures is compared to existing research data? A numerical model for ASR cracking caused domain and a layered model created in Chapter 3 is presented in Chapter 4. A variety of strength values and the concrete damaged plasticity model were used to implement the model in the industry-standard 3D FEA software ABAQUS. Later, this was followed by investigations on the ASR-induced changes in beams' load-carrying capacity.

Chapter 5 explains how to calculate the maximum flexural strength of ASR affected beams chosen from experimental literature using Layered model approach. This chapter answers two crucial problems, namely (i) how the layered model's ultimate strength capability is computed. (ii) what reduction in strength is seen, when comparing the ultimate strengths of damaged and unaffected beam sections.

In **Chapter 6** conclusions & future works – recommendations are covered.

1.4. Addressing Research Gaps

Following points represent the research gap of this study:

1. This study entails a novel technique of modelling ASR-affected structures by introducing the reduced strength material properties for various layers of a concrete specimen. This study uses a beam specimen that is layer-modelled such that the surface and core of the beam are in separate layers. Such a configuration can anticipate the ASR-affected beam's deterioration with surface macro-cracks.
2. Layered modelling approach is useful in reflecting the deteriorating effects of ASR in a FEM model and by allowing input of reduced strength properties. This process allows us to study the load-carrying capacity of the beam and the effects of ASR on the capacity. In this study, the load-carrying capacity of the beams is studied by modelling the beam specimen from existing experiments and comparing it with the experimental results. This way, a knowledge gap in finding the reduction in load-carrying capacity is addressed in this study based on the novel modelling technique.
3. Structures affected by ASR are prone to cracks and reduced durability. The concrete beams show a reduction in strength. Many experiments have been conducted to confirm the reduction in strength. In this study, the flexural strength computation of the beams is shown based on the layered modelling technique. The strength check is done using the Australian Standard of Concrete Structures AS3600. This computation is based on the theoretical concept of the novel layered modelling technique.

1.5. Research Methodology

In this study, first, a critical review of how ASR affects the strength of concrete is provided. To better comprehend and assess the reduction in properties caused by the significant drop in the modulus of elasticity and compressive strength, a thorough literature review is presented.

Secondly, a novel modelling technique is introduced based on the literature knowledge of the ASR affected Structures. The concept is a novel approach in modelling and analysing an ASR affected structure elements such as a beam.

The novel modelling approach is based on material properties rather than pre-defined expansion or stress field data. Rather, it creates geometry by layering the beam and entering reduced strength properties for each layer, implying the effects of ASR at the structural integrity level. Furthermore, flexural strength can be manually calculated using the model. This modelling approach is novel because of its adaptability and availability for use in both software and manual computing.

For obtaining the desired literature, keywords were used such as "Alkali-Silica Reaction," "ASR in concrete beam," ASR Concrete Beam load carrying capacity," "Finite element modelling of Alkali-Silica reaction," "Effect of alkali-silica reaction on the mechanical properties of concrete," "Assessment of ASR-affected structures," "Flexural behavior of Concrete Alkali-Silica Reaction," etc. Also, because a major portion of the Literature review is based on experimental data that can be utilized for modelling and validation, terms such as "Four-point bending test," "simply supported beam model," "experimental investigation," or "experimental study," etc. were also added in the keywords search. Advanced search filters were used, to find the exact match of words. Boolean operators such as AND & OR were used with keywords for e.g., “(Experiment OR Finite element modelling) AND ASR concrete beam”. For the research, databases such as ASCE Library, Scopus, and ProQuest Science & Technology were used, and journal articles were searched through ScienceDirect and Elsevier. The language was restricted to English, and no restrictions were set for geographical locations.

To filter the searched literature, the time frame was set from recent years up to 20 years backdated. The publications were searched based on keywords. Also, publications were searched based on Authors as well, for example, R.N. Swamy, R. Esposito, S. Multon, N. Gowripalan, T. Ahmed, etc. who have published great deal of papers in the ASR related research in concrete. One of the most crucial subjects was to find literature that contained studies based on Finite Element Analysis, especially, studies containing Finite Element beam models. Such literature was extracted and shortlisted from the search.

For extracting the data, I thoroughly researched the papers and extracted information related to the subjects such as ASR development, factors that initiate and progress ASR, experimented data involving beams, comments on ASR mechanisms, comments on the Ultimate strength capacity of ASR-affected beams, etc. These points were utilized to extract the most important information from the sources. This information founded the basis of ASR modelling theory and novel modelling techniques. The modelling approach utilized in the previous research helped us understand the factors influencing the model. All the literature was peer reviewed by Supervisors and based on their feedback, I selected the most recent and most relevant literature.

Finally, using a Finite Element Package 3D ABAQUS 2017 is employed to model based on literature experiments, i.e., Takahashi et al. (1997) and Morenon et al. (2019) and study the results. The numerical models are developed by dividing the cross-section of the beam into four enclosed layers. Each layer will have a different modulus of elasticity. The model is developed using properties such as Elastic Modulus, Poisson's Ratio, Compressive Strength, Tensile Strength, Concrete Crushing Stress, Steel Elastic Modulus, Yield Stress, etc, and the concrete damaged plasticity data. Loss in strength properties and damaged data introduces the ASR effects similar to having expansion data or pre-defined stress- strain data. This way, the model is prepared and tested using similar properties & loading as well as support conditions and compared to the original experimental results. This modelling arrangement makes this modelling technique *novel* because FEA macro-level beam models with cross-sections divided into layers, each layer having

different strengths, are analyzed, and the same layered models are used for computing flexural strength based on a Design Code.

Four-point bending beam data from the literature is used as the fundamental model. It is a frequently employed test that can evaluate both bending and load capacity. Four-point bending is more dependable with the non-homogenous material as a result of the action of ASR and is thus used in this situation. The beam is set up with simply supported beam support conditions, with pinned support at one end and roller support at the other. Two forces are applied at the centre, at some distance apart. The beam is idealistically represented in ABAQUS for this investigation because there are no imperfections or notches.

As a result, in ABAQUS, the displacement, strain, stress, and other parameters are symmetric. The modelling set up is followed by the experimental 4-point bending set up for a simply supported beam model. The beam geometry, mesh, support locations, load locations, load inputs and material consistency are symmetrical. Because of which, the results are obtained as per the reference tests and the bending action as well as the crack formation is similar to the reference tests results. These results are thus, matching with the test results and giving a good agreement. This way the model set up is used to simplify models and reduce computation time.

1.6. Practical Application of Model

The practical approach of the novel modelling technique shown in this study is the design applicability. ASR-affected concrete structures are seen as deteriorating and having reduced strength and serviceability. The effects of ASR cause crack formation and spalling of concrete. It is challenging to incorporate this phenomenon in the design of structures. The layered modelling technique allows the consideration of concrete members and sections in layers, which is feasible in modelling and computing the flexural strength and design of ASR-affected structures. In this study, beams are adapted from the experiments and modelled using a layered model approach. The same beams are used to compute the flexural strength, and reduction is observed.

Layered Modelling approach and its practical application can allow practicing engineers to work out the strength reduction in ASR affected structures.

CHAPTER 2: LITERATURE REVIEW

The state of research on the advancement of alkali-silica reactions in concrete is reviewed in this chapter. Alkali-silica reaction-induced expansion and cracking are two of the leading causes of the degrading of mechanical characteristics of concrete constructions. In the literature, there are many experimental findings that indicate that the ASR affects the reduction of mechanical properties in a variety of ways. One such difference is that the compressive strength of concrete is not reduced to a much lower level as compared to tensile strength and the elastic modulus. The results of the experimental database also demonstrate that, for a given level of expansion, the concrete impacted by ASR degrades to various extents. There are several pertinent aspects that have been connected to the strength loss brought on by the emergence of ASR. When analyzing the ASR degradation, these factors were not taken into consideration or investigated. Moreover, it was discovered that the lower constraints suggested by ISE (1992), which have been frequently used in contemporary practice for evaluating the structural implications of ASR, may be appropriate for tensile and compressive strength only. To gain a fundamental understanding and develop a more accurate estimation model for the degradation of mechanical properties, it is necessary to research further how these factors impact the strength of ASR-affected concrete.

2.1. Alkali-Silica Reaction

Concrete undergoes an alkali-silica reaction as a result of a chemical reaction that is potentially long term. This reaction was initially identified by Stanton (1940). Since then, ASR is known worldwide for causing cracks in concrete structures and is often referred as the “Concrete Cancer”.

The Alkali-Silica reaction consists of two main phases of development:

1) The development of chemical reaction leading to formation of ASR gel.

2) The ASR gel absorbing the moisture and expands, causing crack formation at micro level.

As illustrated in Figure 1, alkali metal ions present in the cement react with the hydroxyl ions present in the reactive silica from certain types of aggregates, which causes the Alkali-Silica reaction.

The gel absorbs water, causing local expansion, leading to internal pressure by swelling, cracking, expansion and reduced strength in concrete members ISE (1992). By absorbing water or moisture, this gel can swell and cause the concrete to expand. The expansion reaches a level where it exceeds the tensile strength of concrete, the crack formation occurs, and cracks tend to grow over the time (Giannini & Folliard 2012; Pan et al. 2012).

There are certain conditions for ASR to take place in concrete. Such three conditions are as follows:

- Presence of reactive siliceous particles in adequate quantity in aggregate.
- Presence of highly alkaline metal ions, sodium (Na) and potassium (K) in cement paste in sufficient quantity.
- Presence of sufficient water i.e., concrete pores possessing 80% or more of the relative humidity.

In the absence of any of the above-mentioned conditions, alkali-silica reaction gel & swelling will not occur.

2.2. Alkali-Silica Reaction mechanism

In general, the alkali-silica reaction in concrete is considered to develop in two different phases. In the early phase, within the surface areas of the aggregates the chemical reaction by-products are formed, and in the later phase, expansion is caused locally by moisture absorption by the reaction by-products Esposito et al. (2016). According to ISE (1992), ASR is a chemical reaction that can occur when specific aggregate components, like silica, are used in concrete mixing and react with alkalis like sodium oxide (Na_2O) and potassium oxides (K_2O) that are dissolved in the concrete pore solution. The chemical processes of ASR are currently poorly understood. There is wide acceptance that the ASR takes place when silica SiO2 in

the presence of water, react with alkalis, which are present in quartz, opaline, or dolomite aggregate and are obtained from cement, admixtures, or external environmental sources Esposito et al. (2016), and for this reason the chemical processes of ASR are currently poorly understood.

The following expression is used to represent the chemistry occurring during the Alkali-Silica reaction and its product alkali-silicate gel:

$$Na_2O + SiO_2 + nH_2O \rightarrow Na_2SiO_3 \bullet nH_2O$$

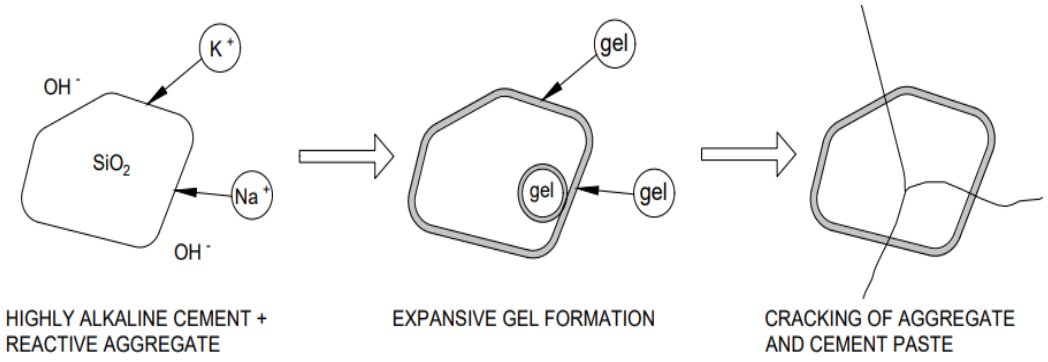

Figure 1. Various stages of ASR damage mechanisms; adapted from Esposito et al. (2016)

As an alternative, if adequate but not excessive crosslinking is maintained between silica chains, a significantly deteriorated (SiO2) solid may directly change into a (SiO2) gel. The dissolution of Silica, which is frequently the slowest of these responses Esposito et al. (2016), so rate of ASR in concrete is primarily controlled by it. For instance, silica dissolving in concrete is increased in accelerated ASR tests by parameters like higher alkalinity and temperature. ASR damage in dry, dense concrete may be limited by swelling of the gel, which depends on moisture availability and mass transport characteristics of the material in addition to silica dissolution. Based on the type of aggregates the formation of the reaction by-product is different. Sanchez et al. (2015) described three distinct reaction mechanisms, including the creation of external reaction rims, diffusion taking place in the aggregates' gel content, and vein forms within particles (Figure 2).

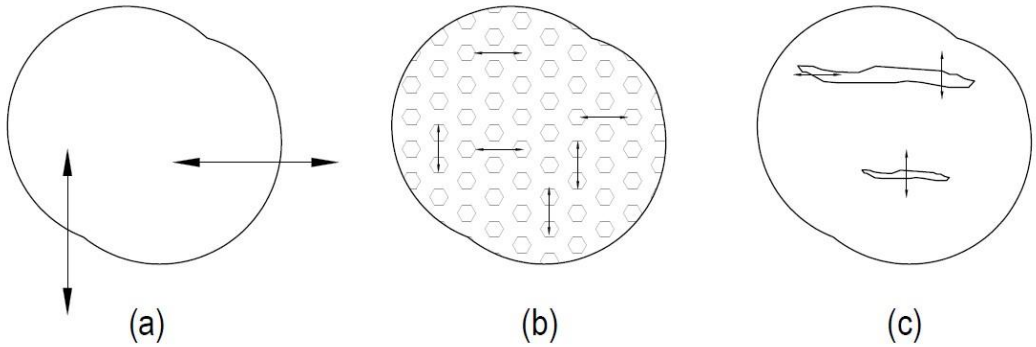

Figure 2. ASR development phases for various types of aggregates; adapted from Sanchez et al. et al. (2015)

2.3 Factors inducing Alkali-Silica Reaction

2.3.1 Temperature

The environmental conditions induce the expansion rate of the ASR, Swamy (1992). When the temperature of the surrounding is at a higher rate, the ASR occurs quicker. Many experiments such as cube compression, tensile splitting test, etc were carried out, with specimens of similar alkali content, at various temperature levels and it was determined that temperature has effect on ASR and concrete expansion. Swamy & Al-Asali (1988) showed by the experiments, that concrete expansion was the highest when the temperature was 38°C. The expansion seemed to decrease beyond this temperature.

2.3.2 Moisture

As the alkali-silica gel expands by absorbing the water, water plays a significant role in the tendency of ASR in concrete. Larive (1998) experimented on concrete cylindrical specimen with a temperature of 38°C. The specimens were kept in different storage environments. Specimen were kept covered by aluminium foil, kept in high & unsaturated humidity (95%-99% relative humidity), in saturated humidity and immersed in water. Expansion in longitude and the water absorption was observed.

It was observed that the cylinders covered in aluminium foil showed the least expansion of 1.0 x 10^{-3} and the specimen kept in 95%-99% relative humidity showed most expansion of 2.0 x 10^{-3}. This demonstrated that the external water intake allows the ASR swelling to expand, however, the structural integrity of concrete reduces even without external water intake. The ASR affected concrete and the non-affected concrete exhibit similar water movement since the water imbibition is the same for the specimen with reactive and non-reactive aggregates.

Multon et al. (2004) conducted experiments on cylinders and beam specimens to investigate the relationship between the ASR expansion and changing moisture conditions. The specimens were kept at different moisture conditions such as one kept full relative humidity and another covered in aluminium foil. Both the specimens were kept in water for two years and bared to relative humidity of 30%. This experiment suggested that the specimen went into larger expansion with later intake of water as the specimen had not reached the maximum expansion potential.

2.3.3 Alkali content

Although it is accepted that the primary source of alkali is Portland cement, numerous other ingredients utilised in the mixing of concrete can also serve as possible sources of alkali, Ahmed et al. (2003). Some of these materials can be admixtures, salt-water of sea, cementitious material, aggregates, etc. $NaO_2 + K_2O$ or Na_2O is the corresponding expression of the alkali presence in the substance. Prior to choosing the type of concrete, it is necessary to consider the environmental conditions where the concrete will be utilised. This is only because the seawater containing the alkali ions is prone to attack the concrete in the form of moisture.

2.3.4 Aggregates and reactivity

The reactivity of aggregates has a great influence on the formation of ASR. The higher reactivity of the aggregates induces ASR rapidly. Although silica is present in many forms of rock, not all the rocks are prone to form ASR. Opal, which is a type of mineral is usually reactive rather than the quartz, which is mostly stable.

In an environment, that contains higher pH, the mineral Opal is highly reactive due to its highly unstable structure. Petrography tests are often used to detect the reactive elements present in the substance.

Along with the alkali content and reactive aggregate, the exposure conditions—temperature and moisture—provide a setting that is conducive to the development of the alkali-silica chemical reaction and the curing of concrete, Smaoui et al. (2005). The primary source of reactive silica for ASR is aggregate. Negative ASR is primarily caused by aggregate size, composition and mineralogy, and maximum reactive contents. The chemical content and appearance of ASR gel, the reaction result of alkali and reactive silica, vary greatly.

2.4. Changes in mechanical properties due to ASR

Concrete structure cracks due to ongoing harmful reactions, which has a negative effect on the mechanical properties of the material. Alkali-Silica Reaction causes the degradation of the concrete mechanical properties which leads to the deterioration of the concrete and the structural integrity of the structure.

Table 1. ISE (1992) Lower bound percentage values of unaffected concrete for residual mechanical properties after 28 days

Property	Strength of concrete in percentage for various free expansion levels when compared to unaffected concrete				
	0.5mm/m	1.0mm/m	2.5mm/m	5.0mm/m	10.0mm/m
Elastic Modulus	100	70	50	35	30
Splitting Tensile Strength	85	75	55	40	*
Uniaxial Compression	95	80	60	60	*
Cube Compression	100	85	80	75	70

* Denotes the unavailability of data for corresponding expansion.

A report on concrete structures influenced by the Alkali-Silica Reaction was published by the Institution of Structural Engineers. This report was issued in 1992

and contains a thorough guidance about the chemical process of ASR, laboratory testing and results, effects on mechanical properties and the discussion on research needs. The lower bound values for various ASR free expansions of those real parameters of unaffected concrete at 28 days are shown in Table *1* as percentages to the mechanical properties of concrete under unconstrained conditions. The values in the tabular data were calculated using lower bounds of laboratory data from tests on prisms, cast cubes and from tests on cores removed from structures.

The lower bound values for tensile strength, elastic modulus & compressive are shown in Figure 3. It illustrates that tensile strength & modulus of elasticity are the properties that are highly affected, even prior to attaining significant expansion, with compressive strength, only higher expansion levels contribute to its reduction.

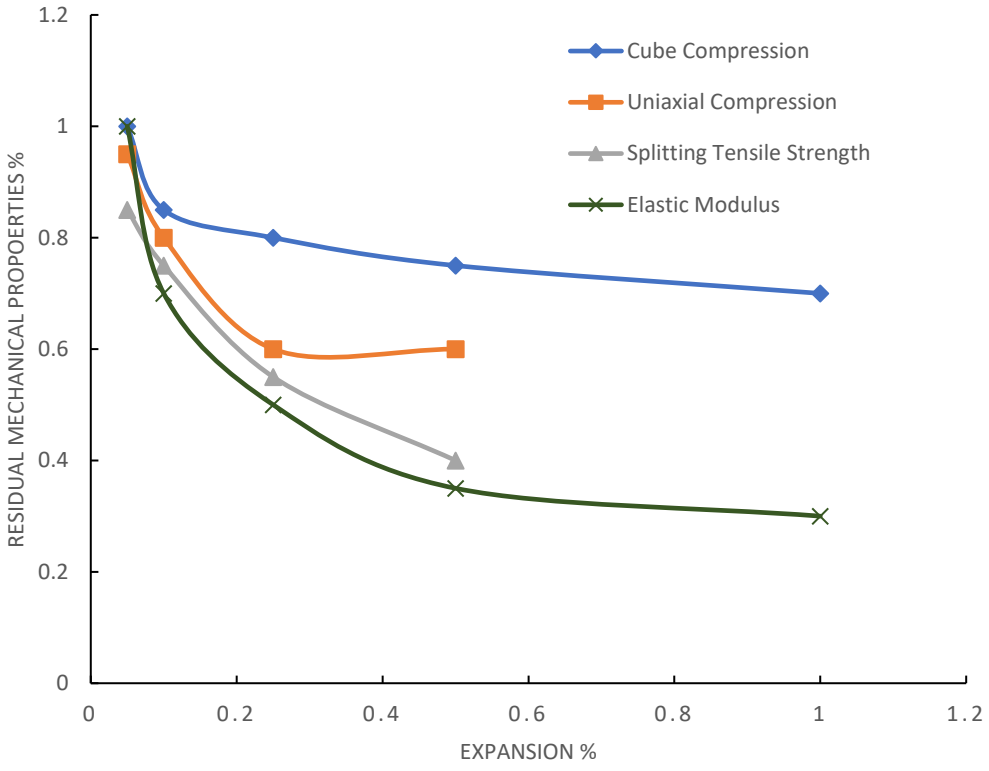

Figure 3. (ISE 1992) Residual mechanical properties against unaffected concrete after 28 days

2.4.1 Change in Tensile strength

The data collected for tensile strength tests; namely tensile splitting test is shown in Figure 4. Numerous experiments indicate that as the expansion level rises, the tensile strength decreases. Concrete cracks and deteriorates due to the severity of the ASR, which results in a reduction in tensile strength. The tensile strength is more sensitive to ASR expansion than compressive strength, according to the strength values. Compared to the unaffected concrete, the tensile strength was found to vary and sensitive for ASR affected concrete specimen.

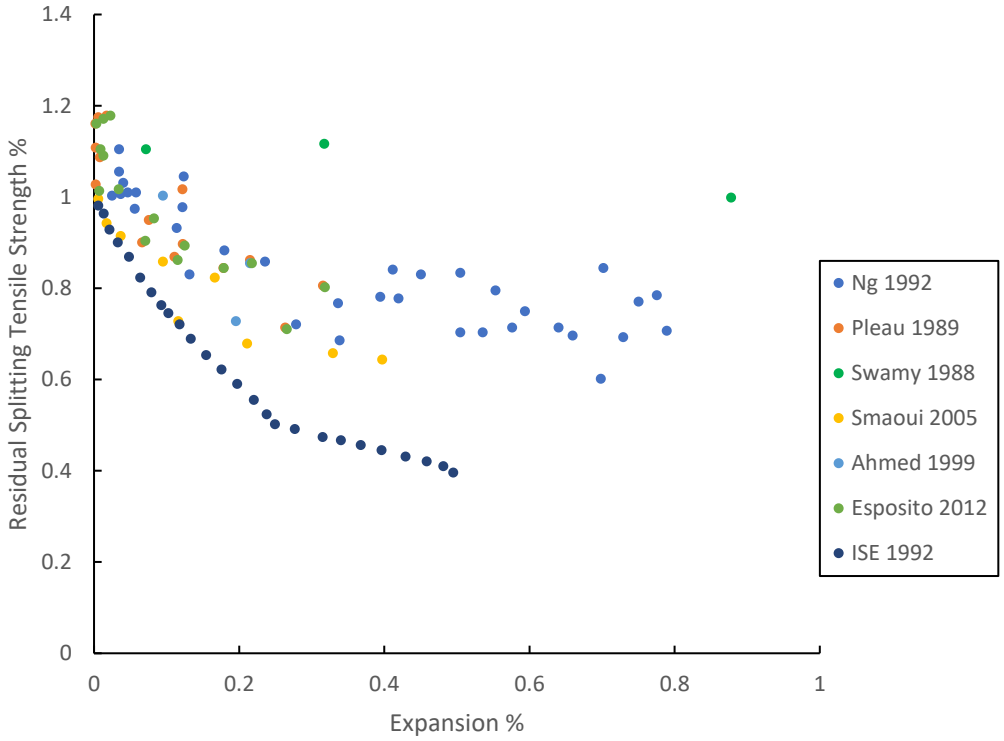

Figure 4. Splitting tensile strength (%) – expansion (%) Nguyen et al. (2019)

From the graph, the tensile splitting test shows greater reduction. The tensile splitting test values significantly decline as the expansion level increases. These numbers pertain to the prism tests that Ahmed et al. (2003) examined and claimed that the direct tensile strength for ASR affected specimen reduced up to 80%. Smaoui et al. (2005) conducted experiments and concluded that tensile strength was the highly affected property and noted a loss of up to 48%. All the tests

demonstrate the higher reduction in the maximum expansion zone, however, the maximum reduction of around 89% is seen in tensile strength, ISE (1992).

2.4.2 Change in Compressive strength

According to the tests carried out to study the reduction of compressive strength, it is seen that there are varying results in reduction. Swamy & Al-Asali (1988). Ahmed et al. (2003) suggested that for indicating strength degradation due to ASR, compressive strength cannot be used. Smaoui et al. (2005) noted that the loss in compressive strength for the tested specimen was only 16%. Giaccio et al. (2008) mentioned that as ASR increases, concrete with reactive particles' mechanical properties deteriorate, but linking these changes to expansion is challenging due to factors like rock mineralogy, aggregate size, and reaction kinetics.

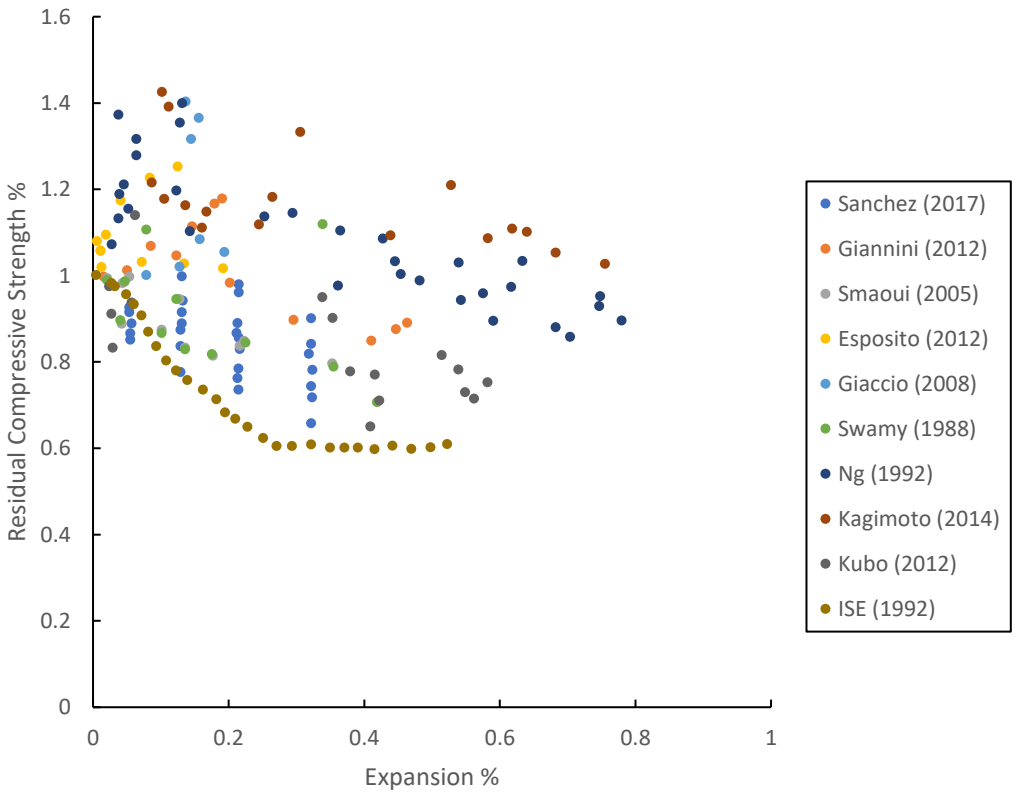

Figure 5. Residual compressive strength (%) – expansion (%); adapted from Nguyen et al. (2019) & Esposito et al. (2016)

Giannini & Folliard (2012) concluded that, although at varying rates, compressive strength typically declined as expansion increased and so it is best to measure elastic modulus directly instead of estimating it from measurements of

compressive strength on a core specimen. The results seem scattered at the low expansion level and in some tests, instead of decrease, an increase in strength is reported. It is inefficient to use design codes to calculate the mechanical properties' values based on compressive strength because other properties significantly decrease when compared to compressive strength.

2.4.3 Change in Modulus strength

Literature data reveals that the change in modulus strength is very sensitive for the ASR affected concrete. The modulus of elasticity changes dramatically and quickly as expansion increases. At an expansion of 1.644%, the modulus of elasticity decreases up to 77% as shown by the results from Swamy & Al-Asali (1988). Ahmed et al. (2003), Giaccio et al. (2008) & Esposito et al. (2016) reported results that showed the decrease of loss in strength is up to 90%.

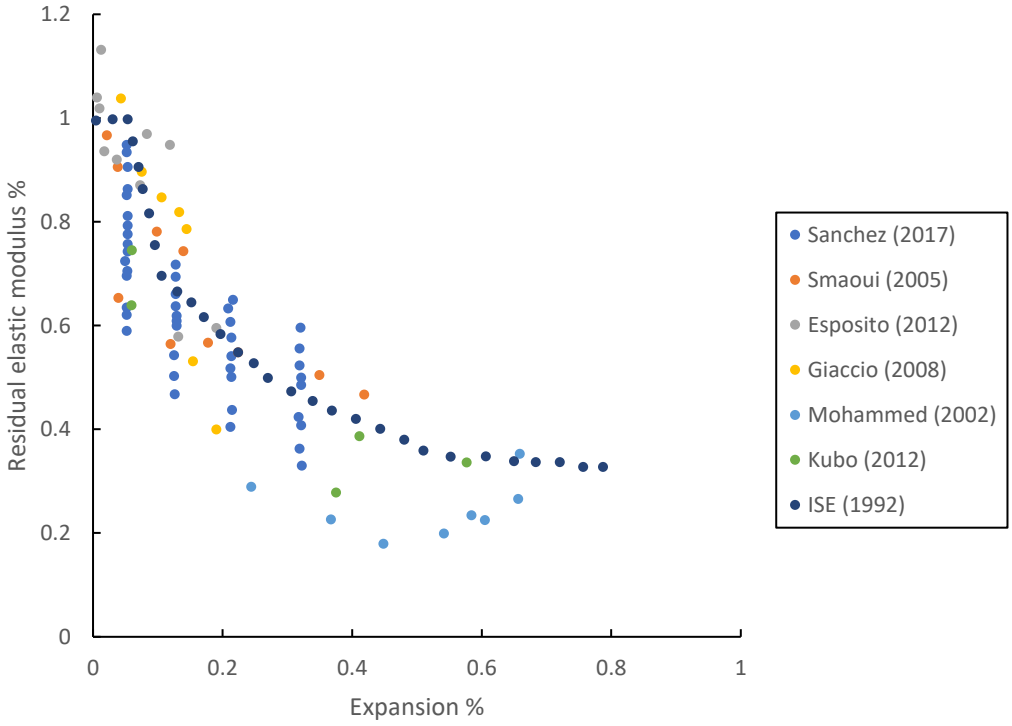

Figure 6. Residual elastic modulus data; adapted from Esposito et al. (2016)

The stiffness qualities degrade similarly at the expansion values of more than 0.10%, as shown in Figure 6. In the extreme-expansion zone, the static elastic

modulus can fall by a maximum of 92% and the dynamic elastic modulus by a maximum of 86%.

2.5. Effects of ASR on Structural Durability & Strength:

Alkali Silica Reaction causes the deterioration of concrete structure by influencing the mechanical properties and strength. Due to which, ASR causes many adverse effects on structure. Some of the effects can be as follows (ISE 1992):

- Macro cracking occurring at surface.
- Changes occurring in the dimensions of concrete.
- Microcracking occurring within the concrete and the expansion occurring in particles.
- Concrete and reinforcement bond stresses.
- Layers of concrete pours experiencing the differential movements.

Some researchers suggested that, based on experimental studies, the flexural strength of ASR affected structures decreases to a significant level. Swamy (1989) reported that a reduction of up to 26% is seen in the concrete beams with only single layer (bottom) reinforcement. Marzouk (2003) conducted tests on concrete beam specimens and reported a decrease of 28% in the compressive strength and up to 80% in modulus of elasticity for concrete with highly reactive aggregates, while a constant value in compressive strength and a reduction of 20% in the modulus of elasticity for moderately reactive aggregates.

Effects of ASR in reinforced concrete is studied by many researchers. Hobbs (1988) found that the reinforced concrete specimens have lesser expansion because the reinforcement causing the restraining effect for the ASR expansions. The area of reinforcement for a concrete section and the positioning of reinforcement can have varying effects causing differential expansions.

The orientation of the produced cracks is caused by the redistribution of concrete expansion. Unrestrained concrete has an irregular crack pattern with crossing and splitting cracks, sometimes known as map cracks (Figure 7a). Appropriate

reinforcements control concrete expansion by arranging the cracks propagating along the direction of the constraint (Figure 7b).

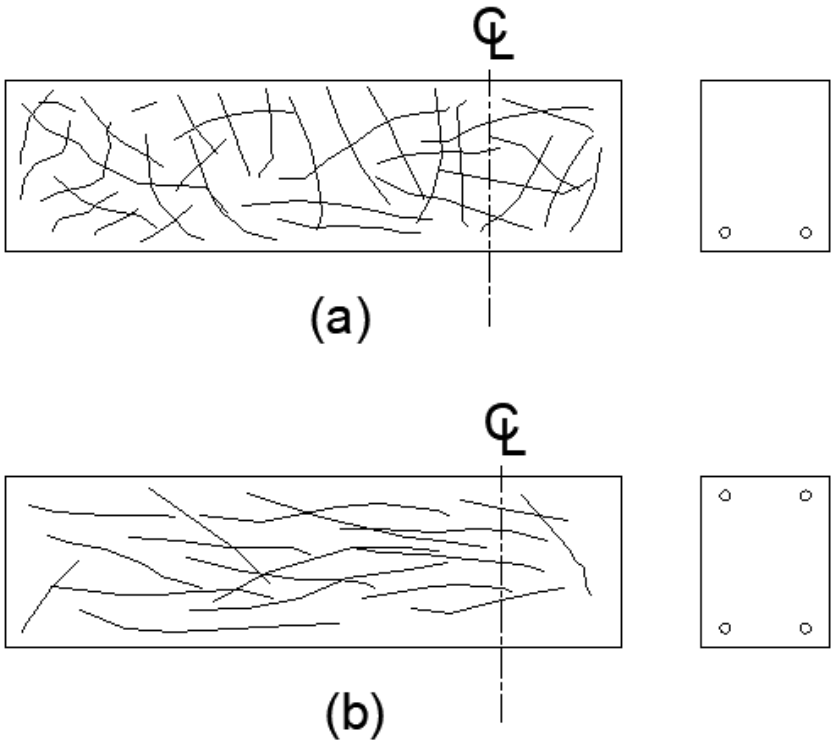

Figure 7 (a-b). Crack patterns of ASR affected beams having: (a) Bottom reinforcement; (b) bottom reinforcement equal to top reinforcement (adapted from ISE (1992)).

Due to which, there is less expansion than in the case of unconstrained concrete. However, the steel bars exhibit tensile stresses, which may cause yielding for lower levels of external loading. The application of external compressive loading has a comparable effect.

2.5.1 Experimental Data on strength reduction in Beam Specimen

Kobayashi (1988) performed experiments on ASR affected beams. In this study, ten prestressed concrete beams made of two types of concrete with alkali silica reactivity (ASR) and ordinary concrete were evaluated for time-dependent strains under fast curing conditions of 40° C and 100% RH.

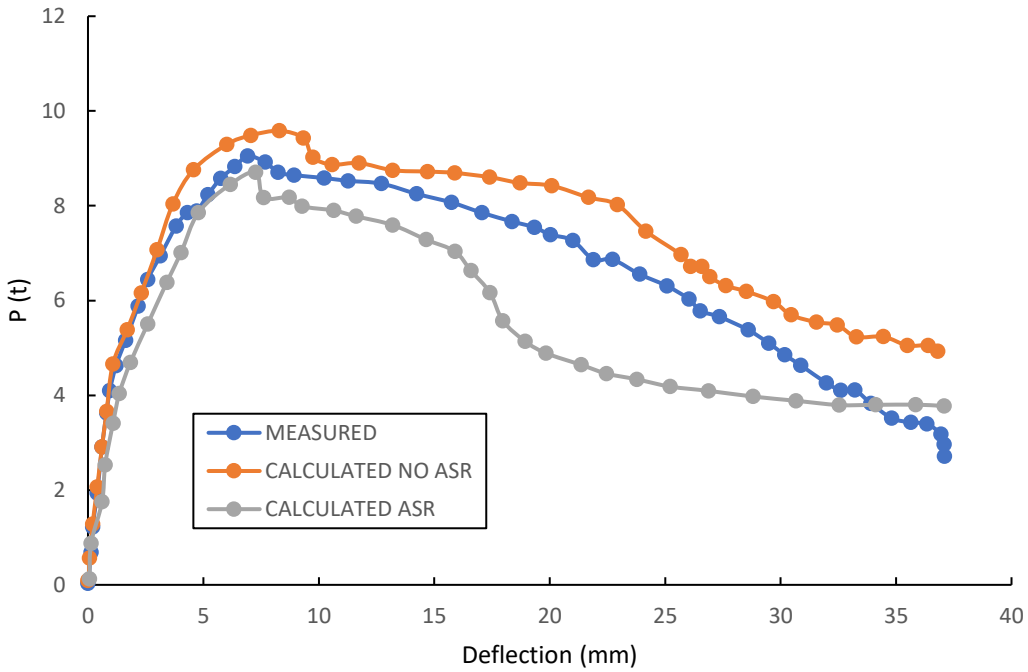

Figure 8. Kobayashi (1988) experimental results; comparison of deflection results

Load vs deflection curve was measured and compared to the theoretically calculated curve, as shown in the Figure 8. Both the curves coincide better than the curve calculated for the ASR affected concrete with reduced compressive strength. As the expanding strain in the vertical stirrup approached 1000 x 10^{-6} and numerous longitudinal cracks appeared, the ASR beam's ultimate strength was reduced by 10% compared to that of a regular beam.

Den Uijl (2000) assessed the behaviour of bridge beams made of flat slabs without shear reinforcement. The shear capacity of reinforced beams is more affected by variations in the tensile strength of concrete. The amount of intact concrete in the beams was just 75% of what was expected. The beams didn't fail in flexural shear as expected, but they did in diagonal shear.

Marzouk (2003) investigated beam specimens with highly reactive and moderately reactive for both the high and normal strength concrete. Author reported a decrease of 28% in the compressive strength and up to 80% in modulus of elasticity for concrete with highly reactive aggregates, while a constant value in

compressive strength and a reduction of 20% in the modulus of elasticity for moderately reactive aggregates.

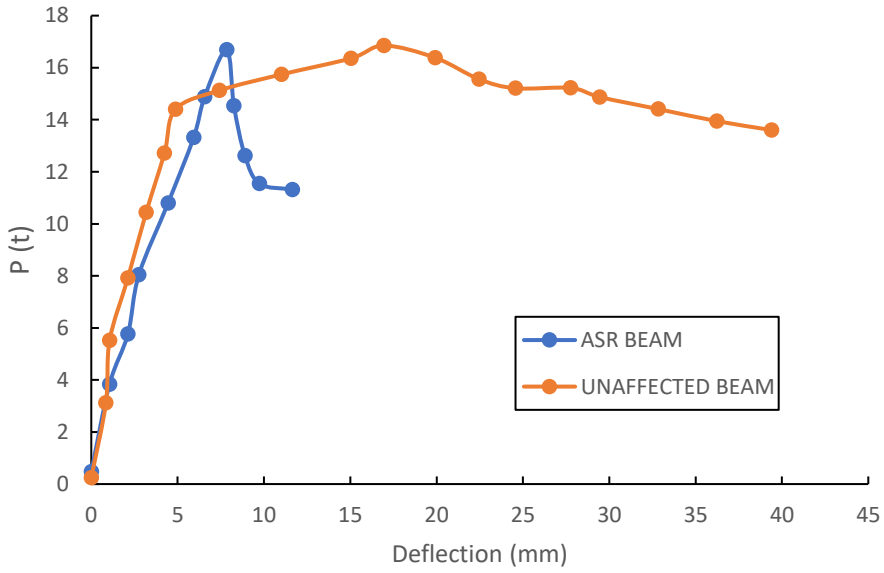

Figure 9. Inoue (1989) experimental results

Inoue (1989) tested beams with various reinforcement ratios i.e., 1.74%, 1.2% & 0.77%. The web reinforcement ratio across all beams was 0.3%. Test results are as shown in Figure 9. It was found that the affected beams possessed lower yield strength and ultimate flexural strengths compared to unaffected beams. A loss of up to 10% for both the strengths was reported. However, it was also found that the unaffected beams failed in shear and in brittle way whereas the affected beam specimen had sufficient ductility, for the case of beams with 1.74% (highest) reinforcement ratio.

2.6 Literature Review Summary

The assessment of expansion due to ASR, property and strength capacity reduction were considerably reviewed in this chapter. Despite extensive research on ASR and its effects over the last 80 years since it was first discovered, determining the effects of ASR in reinforced concrete buildings, and predicting their effects still present significant challenges. The assessment of mechanical property degradation, the modelling of capacity and the prediction of concrete

expansion in field, have been identified as key components for the task of evaluating and predicting the ASR-affected structures.

Research is done to explore the ASR effects on beams by employing numerical analysis using Finite element method. Erkmen et al. (2017) created macro-scale beam model and compared the results with experimental results. Morenon et al. (2019) performed tests on concrete beams and also modelled the same beams using FEA to validate the results. Vo et al. (2021) created macro-scale models and studied effects for up to 45 months for ASR reactive and non-reactive beams. Takahashi et al. (2018) studied the effects of ASR expansion induced preceding cracks on an FEM beam model by observing the strain distribution before and after loading.

The factors affecting the ASR concrete that are highly unexplored are the studies on a beam specimen and comparison between affected and unaffected beams and their flexural capacities. Research needs to be conducted to understand the mechanism of ASR at a structural level for a beam that explains the development and propagation of ASR and its application in modelling and design of beams. A modelling approach needs to be investigated such that it can be applied to day-to-day engineering design and analysis, done by Structural Engineers. For evaluating the ASR affected flexural strength, a theory-based approach is required for the ASR mechanism that can be incorporated into the beam design based on widely accepted literature such as concrete design code; for this research, AS3600. Investigation is required for ASR affected beams and its stress-strain comparison with the existing theory of Equivalent Rectangular Stress Block and commentary on the changes in ASR affected beam based on conventional beam design theories.

The subsequent chapters are written to investigate the strength reduction by ASR and comparison with conventional beam design theory.

CHAPTER 3: MODEL DEVELOPMENT

The literature review addressing the alkali-silica reaction mechanism in concrete and its effects on structures was presented in the preceding chapter. A greater deal of attention must be given to measuring the decrease in concrete's strength properties caused by ASR, as was addressed in Chapter 2. This chapter's literature overview is strengthened with examples of practical approaches, and the idea of creating a layered modelling approach is explained.

The most important research question addressed in this research is**: How can material properties be used to introduce ASR effects in a concrete beam model? And how to develop a modelling technique using material properties to assess the Ultimate Flexural capacity of the ASR-affected beam.** To understand the influence of ASR reaction on the strength capacity of concrete members, it is important to develop a model to obtain long-term ASR effects and the extent of strength reduction.

In this chapter, the following sub-objectives are discussed that serve the purpose of the research: (i) how ASR-induced cracking causes the differential expansion and deterioration of a beam cross-section and (ii) How the ASR-induced cracking mechanism is modeled into a layered beam model.

ASR is a phenomenon that is multiscale in nature and that is why the problem has been studied widely by many researchers by developing models with different functions & aims. This research employs Macro scale modelling because of its ease of using the mechanical property value to assess the problem at structural level and to find the loss in strength.

3.1 Macro scale modelling

In this research, macro-scale modelling is chosen because this research focuses on the ASR problem at a structural level and is related to the flexural strength capacity of a beam element, for which macro-scale modelling is most suitable. The crack development mechanism resulting in the reduction of mechanical properties discussed in Chapter 2 and the layered modelling approach shown in this Chapter are easily applicable to the numerical model at the macro scale. To comment on

the flexural strength loss and to compare it with experimental results, macro-scale modelling is utilized. The ultimate flexural capacity will be computed based on the design code. The alkali-Silica reaction forms a gel product, and the swelling of this gel product induces expansion in the affected portion of concrete, which leads to cracks & deformations. ASR gel formation & development can be prevented by using non-reactive aggregates or cement in the construction activities for the new structures. However, for the current structures affected by ASR, a detailed evaluation of structural performance should be carried out that would reflect on the deterioration of concrete & its properties, which pose a greater impact on the structural performance of the structure.

ASR is a chemical reaction, and reaction kinetics happens to be one of the essential components in modelling ASR. The temperature, moisture content, alkali content, and reactive aggregate types are only a few of the many sub-components that make up this component. The degradation of concrete's mechanical properties is another crucial aspect of ASR modelling, and it often focuses on the deformations, stresses, and material property degradation brought on by the expansion brought on by the swelling of ASR gel.

Macroscale models are very convenient in predicting the global behavior of structures affected by ASR. These models' frameworks enable the introduction of the notions of stress, strain, and deterioration. Charlwood et al. (1992) is a review of a model that focused on the strains induced by ASR & how it affects the structure. Erkmen et al. (2017), Morenon et al. (2019) & Nguyen et al. (2019) studied the effects of ASR at the structural level by creating macro-scale beam models using a finite element modelling approach. Vo et al. (2021) created macro-scale models and studied effects for up to 45 months for ASR reactive and non-reactive beams. Takahashi et al. (2018) studied the effects of ASR expansion-induced preceding cracks on a FEM beam model by observing the strain distribution before and after loading.

In this research, we will only focus on strength properties-based modelling, such as using modulus of elasticity, compressive strength, concrete damaged plasticity data, concrete crushing stress, etc. These properties are researched through the

literature review, experiments are available to suggest how the properties are affected by ASR, and previous experimental studies have researched concrete macro-scale models to find the strength loss by introducing ASR effects using these properties. Moreover, it is very suitable to carry out macro-scale modelling using these properties for a concrete beam model.

3.2. ASR affected Structure and the Deteriorated Layers

In comparison to the 28-day relative value, the concrete specimens subjected to ASR showed decreased compressive strength, tensile strength, and elastic modulus (ISE 1992).

The expansive cracks formed by ASR can cause considerable reduction in elastic modulus and compressive strength, as also has been mentioned by many researchers after performing experiments.

An illustrative model, adapted from Sanchez et al. (2015), shown in Figure 10, depicts the process of crack initiation and propagation for the concrete matrix affected by ASR expansion at an aggregate level and describes how the crack propagation drops the mechanical properties. The highly affected or the early affected property is the elastic modulus. Compared to compressive strength, as can be seen in Figure 10, the elastic modulus is reduced by 30% at only an expansion of 0.05%.

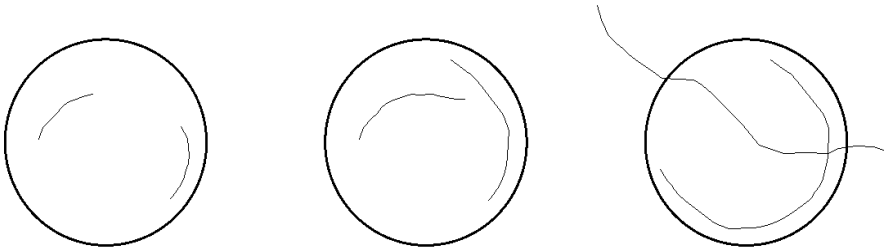

EXPANSION	0.05%	0.010%	0.030%
COMPRESSIVE STRENGTH	100%	90%	60%
ELASTIC MODULUS	70%	65%	50%

Figure 10. Changes in mechanical behaviour and the formation of ASR expansion cracks; adapted from (Sanchez et al. 2015)

The cracks are formed and propagate between the cement phase and the aggregate because the excessive expansion causes the hardened concrete to crack

because the tension created by the expanding force is greater than the concrete's tensile strength, Pan et al. (2012) & Giannini & Folliard (2012). The cracks are formed and propagate between the cement phase and the aggregate at an expansion level of 0.012%. At this phase, a drop of 10% and 35% is seen in the compressive strength and the elastic modulus, respectively. As the cracks expand by 0.2%, their size and form continue to increase, seeping into the aggregate and lowering the elastic modulus to 50% and compressive strength to 75%. Eventually, as the expansion keeps on increasing, the cracks network is developed through interconnection and leaves the elastic modulus and compressive strength of 40% and 60%, respectively. At further expansion, the modulus of elasticity decreases while the compressive strength does not decrease further.

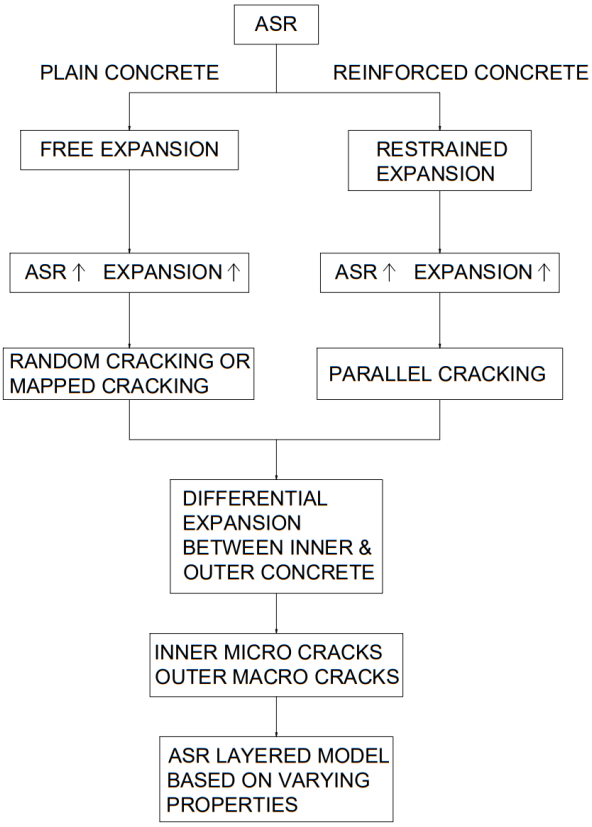

Figure 11. Main principles of Layered Modelling concept

The fundamental ideas of this layered modelling approach are presented in Figure 11, together with the model development concept. The ASR-affected unreinforced and reinforced concrete, respectively, exhibit free expansion and controlled expansion. As the ASR aggression rises, the concrete's expansion rises as well,

creating fissures. For plain and reinforced concrete, the cracking patterns differ. Plain concrete undergoes a random cracking pattern, also known as mapped cracking or unrestrained cracking. However, reinforced concrete shows crack formation, which is parallel to the reinforcement, ISE (1992).

The ASR has enough moisture consumption, and the expansion increases such the crack formation is visible on the surface due to higher tensile strains, Courtier (1990). The layered model concept, therefore, accepts the construction of layers within the concrete based on strength loss, with the outermost layer having the lowest strength due to higher tensile strains.

3.3 Adaption of Model

The literature gives information on how the strength properties of the ASR-affected concrete are proportional to the internal and surface cracks. For the concrete beam affected by ASR, the section of the beam can have varying layers of moduli due to the presence of micro and macro cracks in the core and the surface of the section, respectively. Hiroi (2016) mentioned that the concrete compressive strength is affected by the presence and development of cracks in the concrete matrix. Although the strength reduction is not linearly proportional to the ASR crack development, the decrease in strength is observed as the ASR severity increases, ISE (1992).

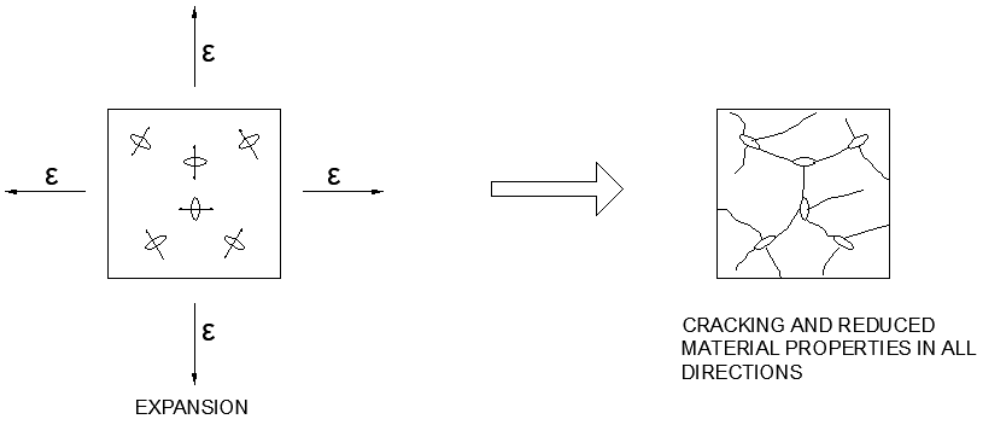

Figure 12. Expansion phenomena for ASR affected Concrete, Esposito et al. (2016)

As also shown by Courtier (1990), the stress and expansion development in the concrete due to ASR is directly proportional to the reduction in strength of concrete and surface macro crack development. As shown in Figure 12, the internal stress conditions affect the boundary conditions and the dimensions of the structure. Due to this reason, for any damaged structure, it is observed that the surface cracks are more severe than the internal cracks, Multon et al. (2006).

3.4 Literature Review on Layered Modelling Technique

The following investigations predict the nature of ASR expansion and cracking phenomena and how they can be incorporated into a design concept.

1) Stark (1991) – According to extensive field research by Stark (1991), there were wide variations in the thicknesses of layers closer to surface in concrete buildings that were already impacted by ASR and had values lower than 80% for relative humidity. The layers which are non-reactive limit the expansion of the inner concrete, causing tensile stresses to build in the domain. Surface cracking could happen from these tensile forces escalating to a certain point.

2) Kawamura (2007) – In a study by Kawamura (2007), it was observed that the maximum tensile stresses that can be created in the layers that are less reactive in concrete cylinders impacted by ASR are calculated in order to predict the critical free expansions for surface cracking. If the depth of the non-reactive layers, the elastic modulus and compressive strength of the concrete, and the sizes of the specimen are known, a simple calculation can be used to determine the critical free expansions for surface cracking in ASR-affected unreinforced concretes. This is predicated on the idea that free expansion is inversely related to expansive pressure and that the non-reactive near-surface layers constrain the growth of inner cores.

3) ISE (1992) – The findings from the report are as follows:

1. Over the entire volume of the concrete, expansion is not constant. Around a group of such particles or in the near proximity of each reactive particle, it is higher. Microcracking could develop from the resulting differential

effects. Furthermore, because of restraints and effects at the outer edges of the concrete mass, the microcracking does not spread equally.

2. Macrocracks rarely extend deeper than the lesser of the cover and around ten percent of the member thickness, or they only marginally affect surface width.

3. A single surface crack multiplies into branching, finer cracks, which then converge into microcracking, as demonstrated by the sectioning of members from demolished structures. Reinforcement efficiently inhibits the spread of surface cracks. Microcracks are often concentrated in the plane of the steel's surface layer due to the constraint. This could progress to more serious deterioration cracking.

Summary: ISE (1992) explains that the expansion is not constant throughout the section of a concrete member, the depth of the surface macro cracks can be assumed to be a tenth of the section dimensions, cracks are restricted with the presence of reinforcement and the surface cracks and inner micro-cracks form a branching structure.

4) Courtier (1990) – The findings from the author are as follows:

1. Courtier (1990) suggested that due to the production of expanding products at specific reaction sites or surfaces, ASR has two major structural impacts. (a) The development of new micro cracks or the escalation of pre-existing ones in the concrete matrix, which results in a slower increase in strength than usual and, in certain cases, a genuine decrease in strength over time. (b) The expansion of the concrete's body, which creates restraint forces both inside the body's internal non-reactive zones and anywhere else it interacts with other materials, such as reinforcement or other structural components.

2. Cracks typically only penetrate close to the "neutral axis" that separates the expansive and less expansive sections and not across it.

3. The contact between the core and the surface directs surface cracking. The matrix will take advantage of the weakest stress field in order to respond to local expansion under a compressive stress field on the heart concrete. This will prevent concrete from expanding in the direction of the applied field, and any micro-cracking that does occur will likely take place parallel to the applied field and produce an expansion that is normal to it. On the other hand, regular microcracking will take place in this field if a tensile field is applied.

Summary: Courtier (1990) explains that the expansion is not constant throughout the section of a concrete member, the depth of the surface macro cracks can be assumed to be 10th of the section dimensions, cracks are restricted with the presence of reinforcement and the surface cracks and inner micro cracks form a branching structure.

5) Kagimoto et al. (2014) – For the purposes of optimizing the calculations for ASR-induced expansion, the internal RH of large concrete specimens exposed in the field is initially assumed to be 100%, applied uniformly throughout the specimen, and constant during the course of exposure. The expansion of the blocks exposed to field and RH sensitivity is regarded as a study of parameters. Only the cover of concrete members is impacted by ambient RH, and while the inside concrete layer takes years to reach equilibrium with the surrounding air's relative humidity, the interior concrete core is still saturated.

6) Kongshaug et al. (2020) – An anisotropic stiffness decrease is seen for restrained specimens, which is similar to the expansion behavior. A lesser drop in elastic modulus is discovered in the direction of loading (Z) than in the free directions (X and Y). One causative variable, namely the expansion in the same direction, accounts for the lowering of the elasticity modulus in a specific direction. The expansion mechanism for a ASR affected concrete beam section is shown in Figure 13.

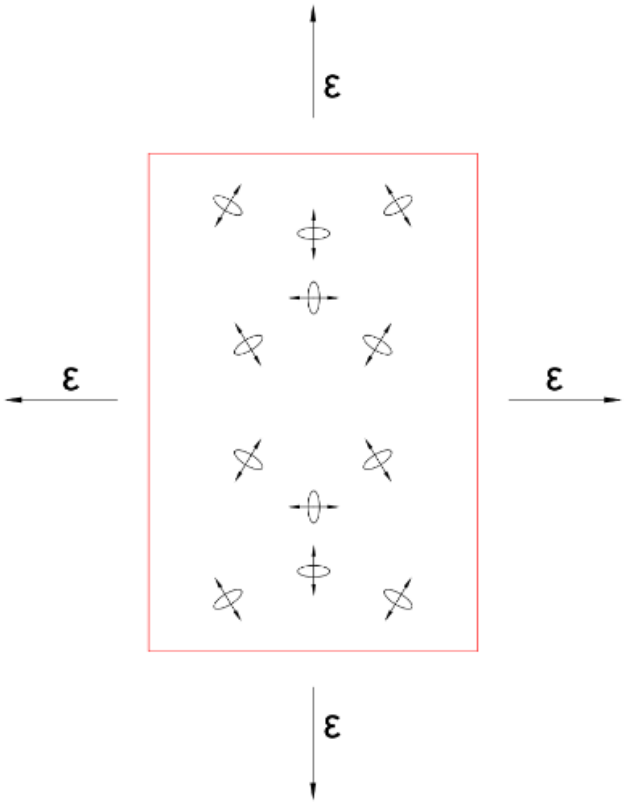

Figure 13. Expansion for ASR affected Concrete Beam Section.

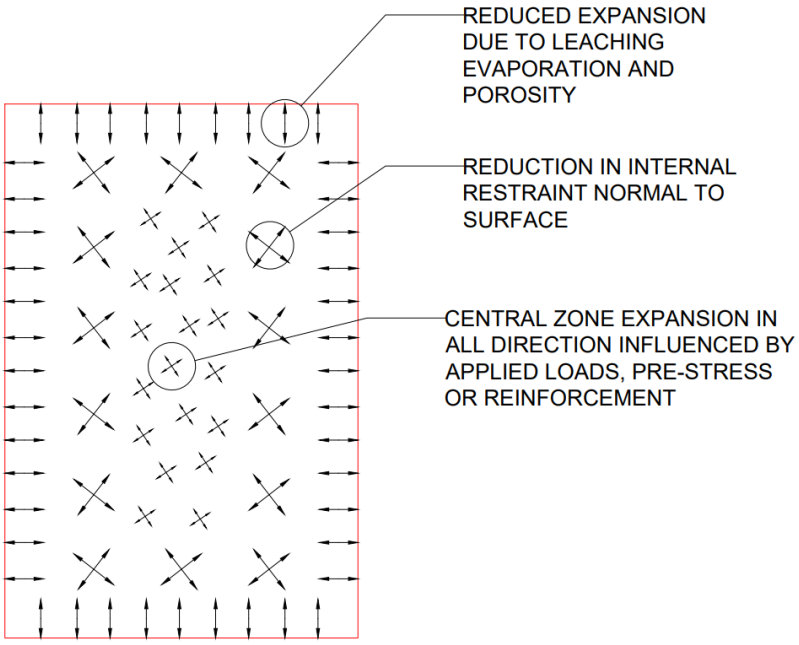

Figure 14. Differential Expansion for ASR affected Concrete Beam Section, Courtier (1990)

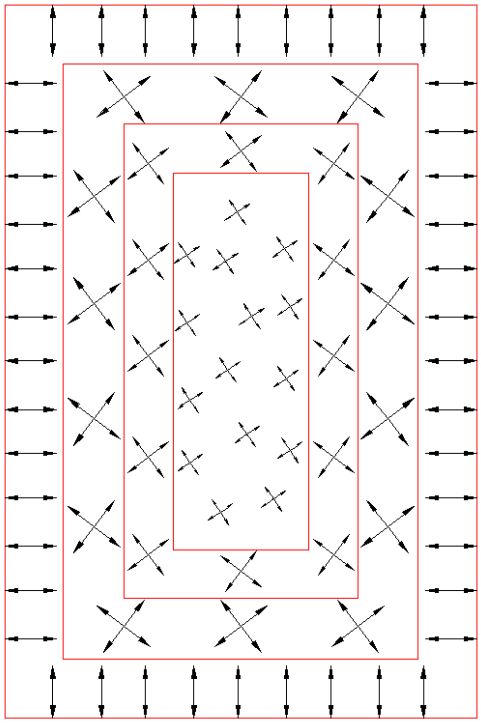

Figure 15. Layers of Differential Expansion for ASR affected Concrete Beam Section, Courtier (1990) & ISE (1992)

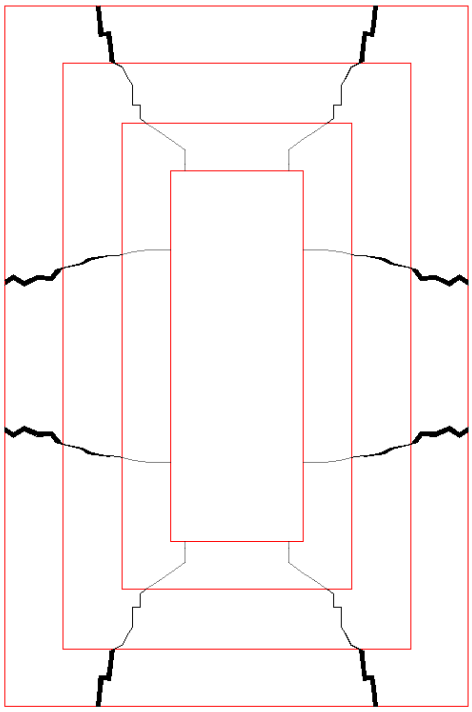

Figure 16. Differential Cracking of ASR affected Concrete Beam Section, Courtier (1990) & ISE (1992)

The ASR phenomenon and crack formation for a concrete beam section are illustrated in Figures 13-16. According to the literature review, a beam segment may experience differential expansion. Since the expansion is in all directions that are free, layers can be assumed. Based on the difference in tensile strain between the inner and outermost concrete, this assumption can be confirmed. Because of this, cracking formations develop, making wider or more severe cracks apparent on the surface. At the core of the section, these cracks can be seen closing and branching into microcracks. The core idea behind the layered modelling approach is this fundamental concept.

3.5 Conclusion

The macro cracks on the concrete surface, are greater than the internal micro cracks, which leads to considerable amount of loss in strength for the outermost concrete fibres compared to the internal.

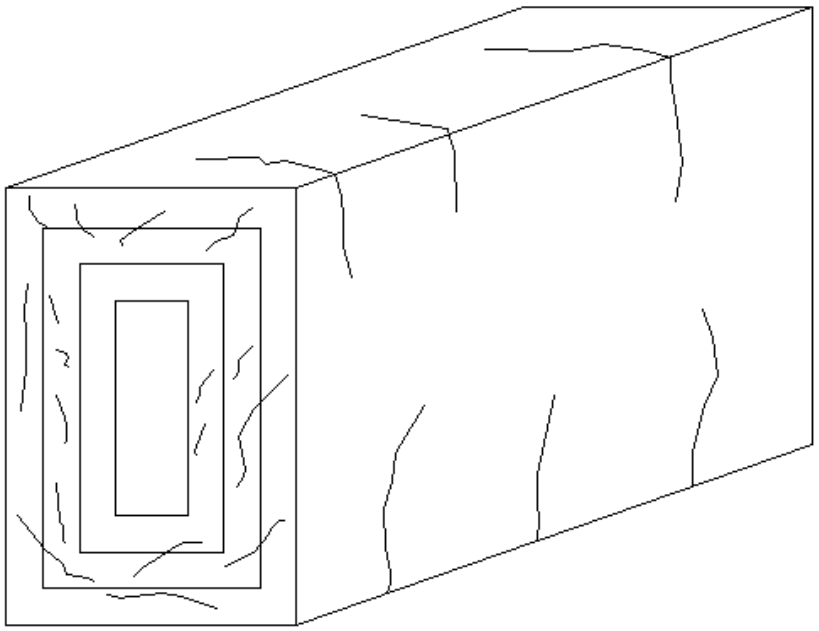

Figure 17. Development of Macro-cracks in a beam section

This phenomenon can mean that the cross-section of the ASR-affected beam has varying strength, with the outermost fibers having lesser strength due to the macro crack development. The varying and differential expansion at the core and the surface of the concrete causes the surface cracks. The formation of significant

macrocracks on the outermost layer of a beam section is shown in Figure 17 as a layered model. As we move towards the innermost layer of the section, the severity of the number of cracks and their size lessens, as shown by Courtier (1990) in Figure 17. As a result, considering the theory of layers of strength is authenticate & useful for constructing and developing an ASR model.

CHAPTER 4: NUMERICAL MODELLING

Chapter 4 widely presents the development procedure of a FEM model based on the reduction in mechanical properties due to ASR. The layered model is investigated analytically and statistically in the preceding chapter, but there is no comparison made. The proposed model is used in this chapter to simulate the behavior of concrete members using benchmark experiments Takahashi et al. (1997) & Erkmen et al. (2017) and Morenon et al. (2019). In this research, two types of models were developed. FEM Model-I type is modeled based on the beam specimen tested and modeled by Takahashi et al. (1997) & Erkmen et al. (2017), respectively. Model-II type is modeled based on the FEM models of Morenon et al. (2019). Both the models are developed with ASR & No-ASR effects. The reason for choosing the experiments is to obtain variety in results. Takahashi et al. (1997) are based on the four-point bending test, and the beam is reinforced with bottom reinforcement only, whereas Morenon et al. (2019) performed experiments on unreinforced and doubly reinforced beams. Utilizing these data, the Layered modelling approach will be able to validate three types of beams: unreinforced, singly, and doubly reinforced beams. To achieve the same results as the benchmarks, the parameters of the model are changed, and damaged plasticity data is adopted to determine the most suitable value for deteriorated concrete due to ASR. The focus of this chapter is to develop the model implement material properties and validate the layered modelling technique by utilizing the reduction in properties based on experiments and literature review.

4.1. Validation Process for Layered Model

The model development and validation are done in the following four steps. Step 1: Determine the material properties from the experiment. The properties such as Young's Modulus, Compressive strength, Yield stress, reinforcement details, etc., are obtained from the literature. Step 2: Determine the concrete-damaged plasticity data based on reference literature. Step 3: Simulate the model based on data and layered modelling approach of reduced strengths. Step 4: Compare results to benchmark Experiments to validate the layered modelling technique.

The material properties are determined from the research papers of Takahashi et al. (1997) & Erkmen et al. (2017) and Morenon et al. (2019). Properties include the modulus of elasticity, concrete compressive strength, Poisson's ratio, steel yield stress, etc. The CDP data is obtained using the CDP model given in the ABAQUS manual.

4.2. Research Model-I

4.2.1 Experimental Benchmark

The first research model is Model-I, which is based on a beam test done by Takahashi et al. (1997). The beam was tested under a 4-point bending test. The beam specimen consisted of only bottom reinforcement. This beam was adapted for modelling by Erkmen et al. (2017). The numerical model of Erkmen et al. (2017) was developed to compare with the original beam test. The beam size, dimensions, load locations & supports in Figure below.

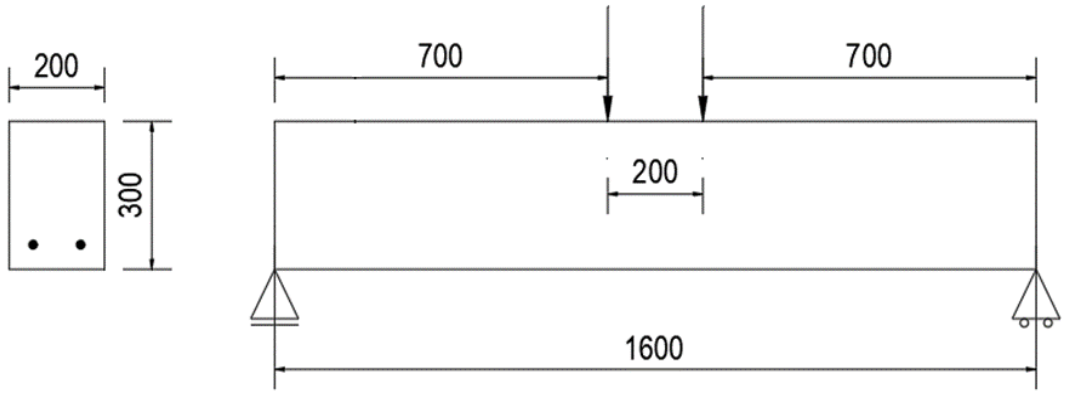

Figure 18. The beam model used for modelling Takahashi et al. (1997) (all dimensions are in mm)

4.2.2 Model-I Geometry

Research Model-I is based on the same beam as tested and modelled by Takahashi et al. (1997) & Erkmen et al. (2017), respectively. The length of beam is 1600mm and the cross section has dimensional width of 200mm and height of 300mm, with

the similar loading load & support conditions. The Abaqus Model-I is shown in Figures 19 & 20.

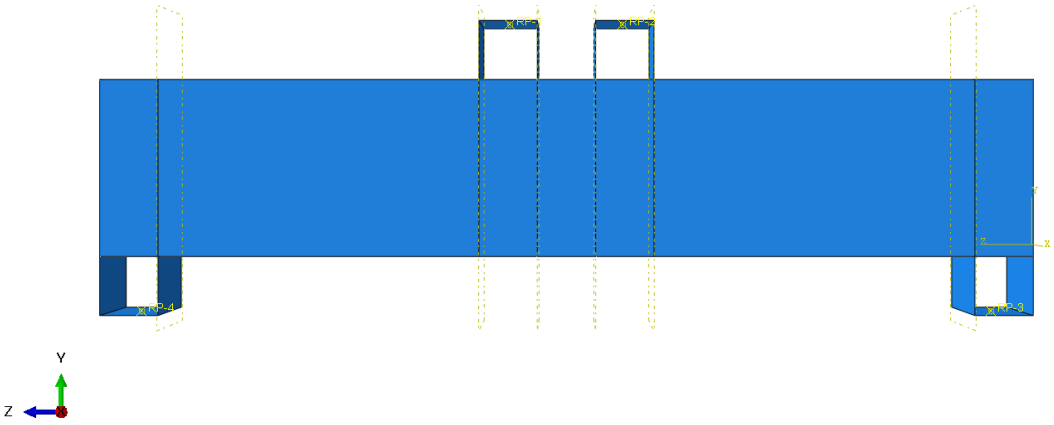

Figure 19. Abaqus Layered beam model, Model-I 2D

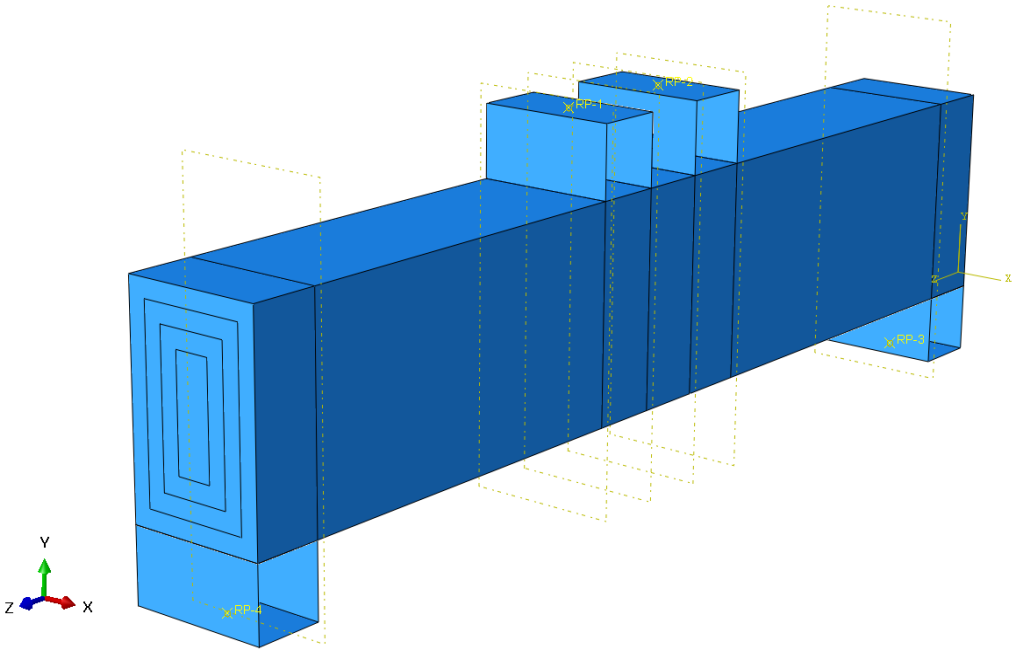

Figure 20. Abaqus Layered beam model, Model-I 3D

4.2.3 Concrete Damaged Plasticity

The constitutive model utilised in finite element modelling of reinforced concrete is presented in this section. The concrete damage plasticity model (CDP), utilised in an FEA software ABAQUS, is used to implement the finite element analysis and it's data is obtained using the CDP model given in ABAQUS manual.

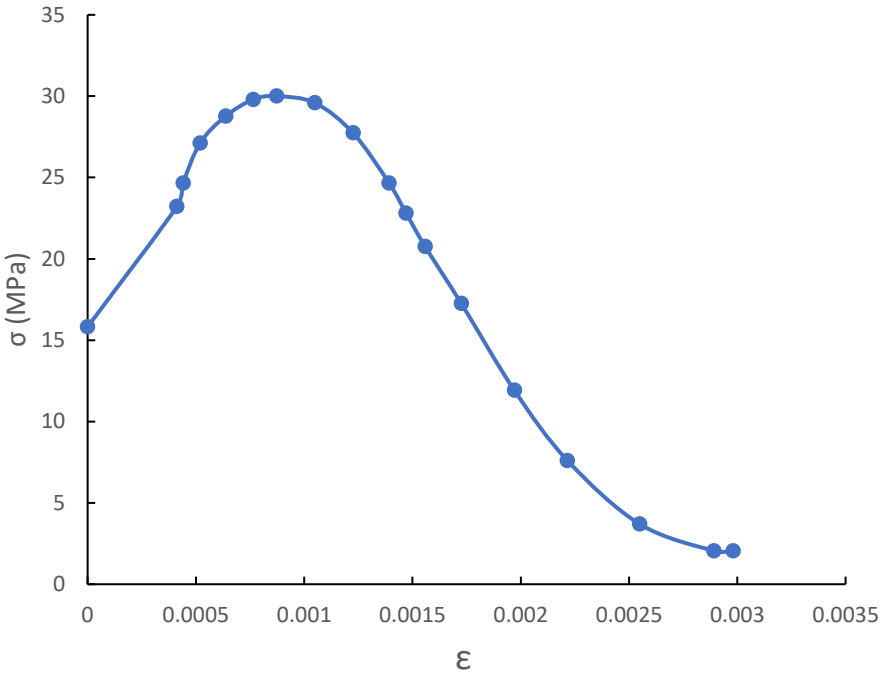

Figure 21. Concrete uniaxial compression loading condition response

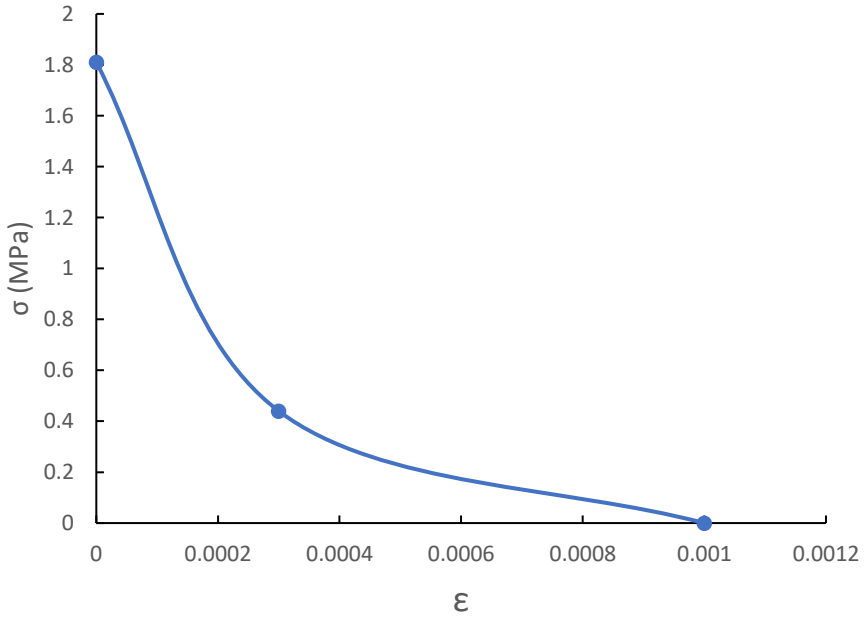

Figure 22. Concrete uniaxial tension loading condition response

The concrete damaged plasticity model in Abaqus is a versatile tool for modelling quasi-brittle materials like concrete in various structures. It uses isotropic damaged elasticity and isotropic tensile and compressive plasticity to represent the inelastic behavior of concrete. It can be used for plain concrete and reinforced concrete structures and can be used with rebar for concrete reinforcement. It requires isotropic and linear elastic behavior data as input. This model is presented by the concrete behaviour of crushing in compression and cracking in tension. This causes the development of yield surface by loss in elastic stiffness, Hafezolghorani et al. (2017).

Uniaxial compressive behaviour is defined by the following:

$$\sigma_c = (1-d_c)\, E_0\, (\varepsilon_c - \varepsilon_c^{pl}) \quad (1)$$

Uniaxial tensile behaviour is defined by the following:

$$\sigma_t = (1-d_t)\, E_0\, (\varepsilon_t - \varepsilon_t^{pl}) \quad (2)$$

where σ is yield stress, d is the damage parameter, E is the elastic modulus and ε & ε^{pl} are the inelastic & plastic strain respectively.

The two primary failure mechanisms of concrete material, presented in (1) & (2) in the continuum and plasticity-based CDP model are either compressive crushing or tensile cracking. The response of the concrete to uniaxial compression & tension loading condition, chosen for Model-I & Model-II for introducing ASR effects for undamaged concrete layer are show in Tables 2 & 3.

For each layer of beam, a separate CDP data is calculated based on the percentage of strength reduction in mechanical properties, and using that data, the layers are modelled, and the beam is analysed.

Table 2. The CDP Data for Compressive behaviour

Young Modulus (MPa)	**Poisson's ratio**		
44500	0.2		
Dilation angle	**Eccentricity**	**fb0/fc0**	**K**
31	0.1	1.16	0.67

Compressive behaviour		Compression damage	
Yield stress	Inelastic strain	Damage parameter	Crushing strain
15.82191781	0	0	0
23.21917808	0.000411765	0	0.000411765
24.65753425	0.000441176	0	0.000441176
27.12328767	0.000519608	0	0.000519608
28.76712329	0.000637255	0	0.000637255
29.79452055	0.000764706	0.006849315	0.000764706
30	0.000872549	3.33067E-15	0.000872549
29.5890411	0.00104902	0.01369863	0.00104902
27.73972603	0.00122549	0.075342466	0.00122549
24.65753425	0.001392157	0.178082192	0.001392157
22.80821918	0.001470588	0.239726027	0.001470588
20.75342466	0.001558824	0.308219178	0.001558824
17.26027397	0.00172549	0.424657534	0.00172549
11.91780822	0.001970588	0.602739726	0.001970588
7.602739726	0.002215686	0.746575342	0.002215686
3.698630137	0.00254902	0.876712329	0.00254902
2.054794521	0.002892157	0.931506849	0.002892157
2.054794521	0.002980392	0.931506849	0.002980392

Table 3. The CDP Data for Tensile behaviour

Tensile behaviour		**Tension damage**	
Yield stress	Inelastic strain	Damage parameter	Cracking strain
1.81	0	0	0
0.44	0.0003	0	0.0003
0	0.001	0.4064	0.001

4.2.4 Model-I Material Properties

Model-I is made up of the Model-I No ASR and the Model-I ASR models. The modulus and plasticity data for the entire section are the same for Model-I without ASR effects. Layered modelling technique has been used with Model-I ASR. The table below shows the material properties selected for the Model-I with and without ASR effects.

Table 4. Material Properties for Model-I No ASR

Model-I No ASR		
Elastic Modulus E	44.5	GPa
Poisson's Ratio	0.2	
Compressive Strength f_{cu}	30	MPa
Tensile Strength ft	2	MPa
Concrete Crushing Stress	10	MPa
Steel Elastic Modulus	180	GPa
Yield Stress f_{sy}	371	MPa

Table 5. Material Properties for Model-I ASR

Model-I ASR		
Elastic Modulus E - Layer 1 - Outermost	22.25	GPa
Elastic Modulus E - Layer 2	30	GPa
Elastic Modulus E - Layer 3	37.5	GPa
Elastic Modulus E - Layer 4 - Innermost	44.5	GPa

For Model-I ASR, the layered modelling approach has been employed. As seen in Chapter 3, sections 3.3 to 3.5, the theory behind the development of the layers in a beam cross-section, the outermost layer of the section, is the weakest due to the development of surface macro cracks. The surface macro cracks branch into micro-cracks as they reach towards the core of the cross-section, because of which the innermost layer possesses the full strength or 100% of elastic modulus. Using the adapted model theory, the Model-I ASR is layered with the different moduli for each layer, with the outermost layer having the lowest modulus reflecting the highest amount of strength loss due to ASR. The outermost layer has a modulus drop of up to 50%.

The thickness of the layer is decided based on the literature ISE (1992) & Courtier (1990) that suggests that the outermost layer with severe large cracks is formed of 1/10th of the cross-section or in other words the first layer can be from the outer edge up to the first layer of reinforcement which is equal to the reinforcement cover. For keeping the section geometry symmetrical and less complex, four layers are assumed, keeping the area of the innermost layer

approximately 15-20%, because, during the ASR-related cracking, the innermost layer can remain intact and uncracked as per Courtier (1990), Stark (1991) & Kawamura (2007). Based on this, the model is assumed to have four layers with equal thicknesses, with each layer having a minimum thickness of almost equal to the reinforcement cover, approximately 20 to 30mm, and the innermost layer having a minimum area of 15-20% of the entire cross-section.

The four layers of moduli are such: outermost is 50% of modulus, i.e., 22.25GPa, and the second layer is approx. 67% i.e., 30GPa, third layer is approx. 85% i.e., 37.5GPa and the innermost layer is 100% i.e., 44.5GPa. The modulus of layers will increase as it goes towards the core, and the innermost layer will have a 100% modulus reflecting the ASR behavior where the cracks and the strength loss due to the spalling of concrete is more on the outside edge than the innermost section of a concrete beam due to more surface tension and larger cracks. The Modulus properties based on layers are shown in table 5 above.

4.2.5 Load Conditions

Model-I is supported in the manner of a simply supported beam, i.e., one end of the beam is pinned, and the other end is supported by a roller. In the displacement control analysis, the top plate's midpoint is subjected to two predetermined displacements, each of which loads the beam, applied statically. Displacement loads are applied statically with the reference points of the loads locked except in the downward direction so that the torsional effect is not created. The non-analytical box pads are used to apply displacement loads. This load arrangement and direction are chosen in the modelling because they represent the 4-point bending test scenario from the actual experiment. Support is first attached in the direction of the load before the prescribed displacement may be attached in the same direction. Degrees of freedom are no longer present in these displacements. The displacement load is applied using a one-step analysis. In the initial step, the displacement loads are not applied, and in step 1, the displacement loads are applied to the specified value. The reference load, in this instance, is directed

downward, and thus, the load application is done in a similar manner as the actual experimental beam test arrangement.

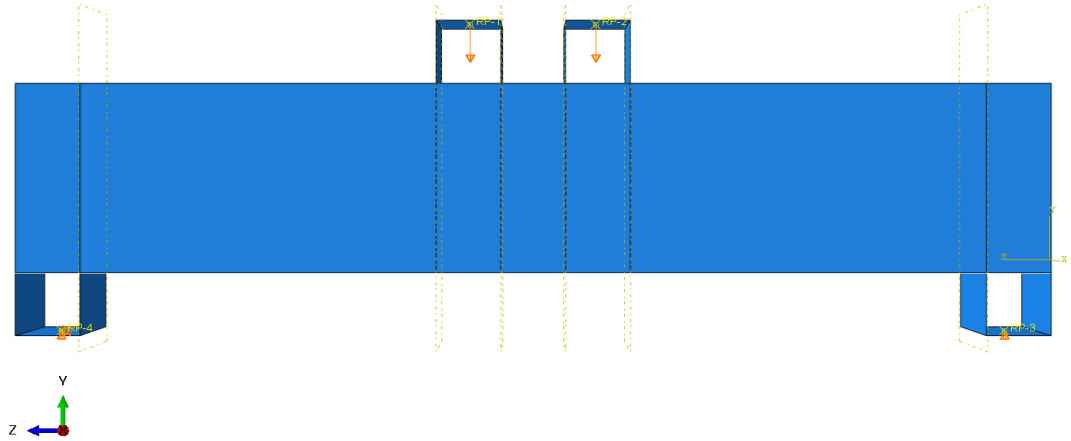

Figure 23. Model-I loads and supports

4.2.6 Validation of Model-I

The Abaqus unaffected FEM model is compared to Takahashi et al. (1997) beam. The load displacement curve shows that the comparison has good agreement as shown in Figure 24. The Takahashi et al. (1997) beam can be seen to fail and deform at reading of 180kN and at a displacement value of approximately 3.5mm.

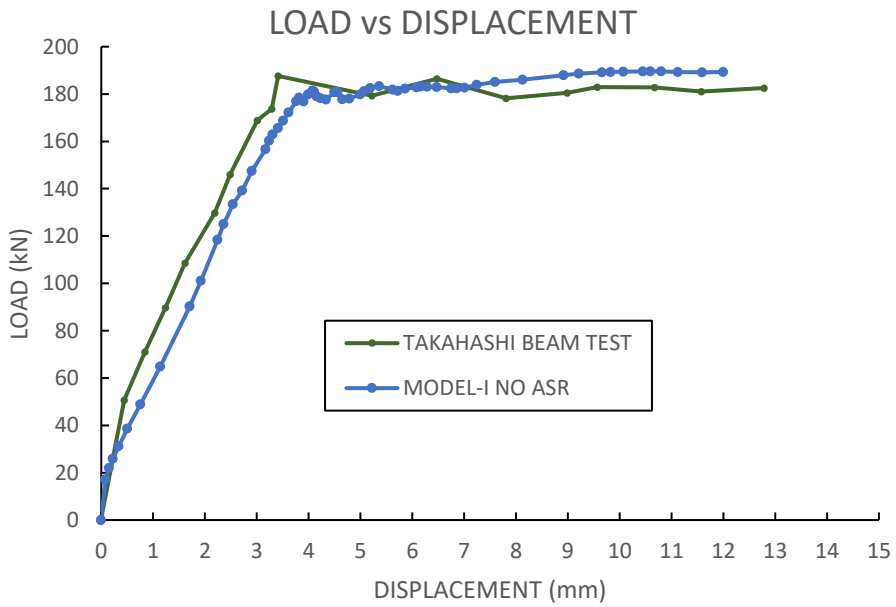

Figure 24. The comparison of Model-I and the Takahashi et al. (1997) Beam load-displacement curve

This comparison between the FEM Model-I and the experimented beams implies that the layered FEM model is able to predict the same behavior and results as the actually experimented beams. Due to this, the layered modelling technique is validated through the validation of Model-I. The Model-I without ASR can be seen to start failing at approximately 180kN and at a displacement value of approximately 4mm. The purpose of the comparison of Model-I No ASR with Takahashi et al. (1997) beam is to implement the first step of model validation by creating the same test model and comparing it with the experimental results before inputting the ASR effects values and creating an ASR version of the same model. The validation of this No ASR Model is to validate that the FEM Model matches the test results of Takahashi et al. (1997) beam test. After this validation, the modelling can continue by inputting the ASR-related data in the FEM Model and comparing the results of the ASR and No ASR models.

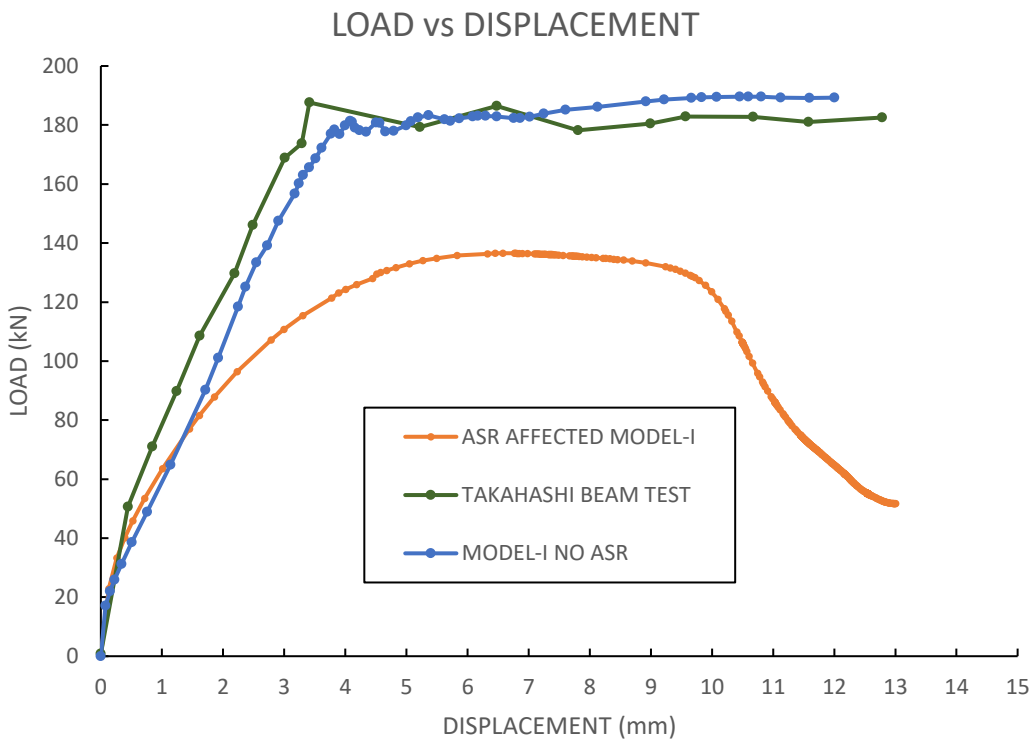

Figure 25. The comparison of Layered ASR model with the Takahashi et al. (1997) load-displacement curve

Model-I No ASR & Takahashi et al. (1997) beam is compared to the affected beam Model-I with ASR properties shown in Figure 25. The comparison shows that with

the ASR values shown in Table 5, the load-carrying capacity is reduced to a certain level. The load-carrying capacity for Model-I ASR is reduced to approximately 130 kN compared to 180 kN for the unaffected beams. This shows that for ASR-affected beams, the load-carrying capacity is reduced due to the formation of cracks and weaker layers on the outer surface. The loss of strength on the outer layers, as shown in the Table 5 data, the concrete spalling, and higher strain values are reached at lower stress levels. Due to this, load-carrying capacity reduces, as seen in Figure 25. The comparison of this Model-I validates the layered modelling technique for singly reinforced beams.

The Model-I mesh arrangement, as well as the Model-I ASR stress and plastic strain distribution, are shown in Figures 26-29. The plastic strain distribution in the longitudinal direction is a good indication of deformities and crack development in the model. The crack development and propagation in singly reinforced beams are random, which means that the areas of the concrete beams where there is no reinforcement are prone to random cracks and greater deterioration due to ASR compared to doubly reinforced concrete, showed in Figure 7 in Chapter 2 (adapted from ISE (1992)). According to Hobbs (1988), the restraining effect of reinforcement causes specimens of reinforced concrete to expand less, with differential expansions being caused by variations in reinforcing area and location.

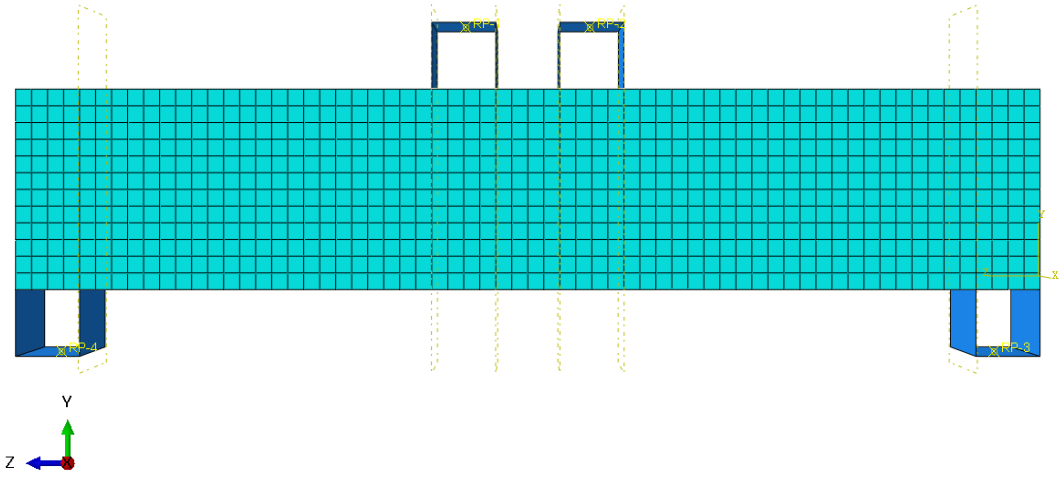

Figure 26. The Mesh arrangement of Model-I

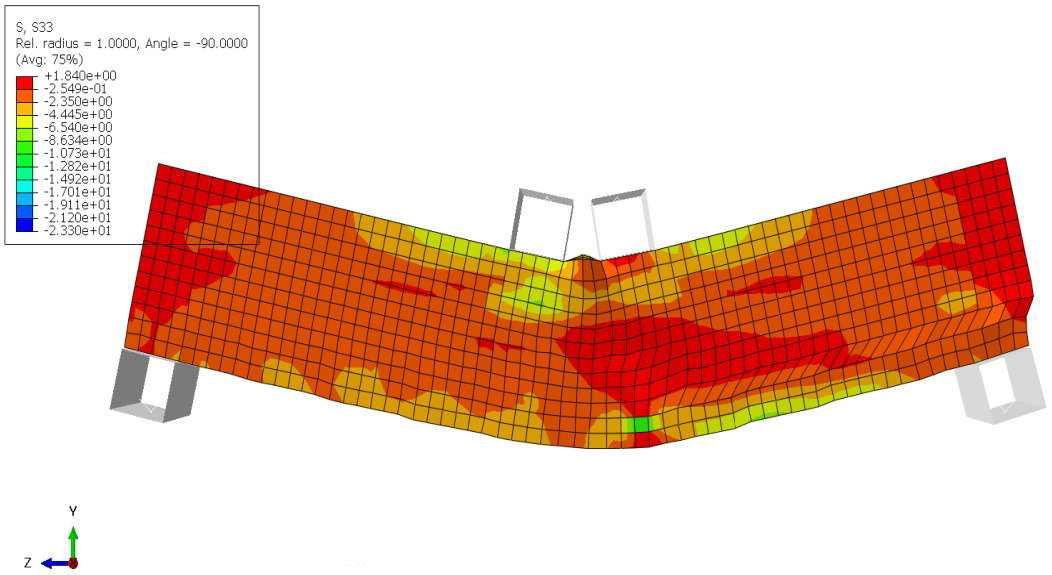

Figure 27. Stress distribution in longitudinal direction for Model-I

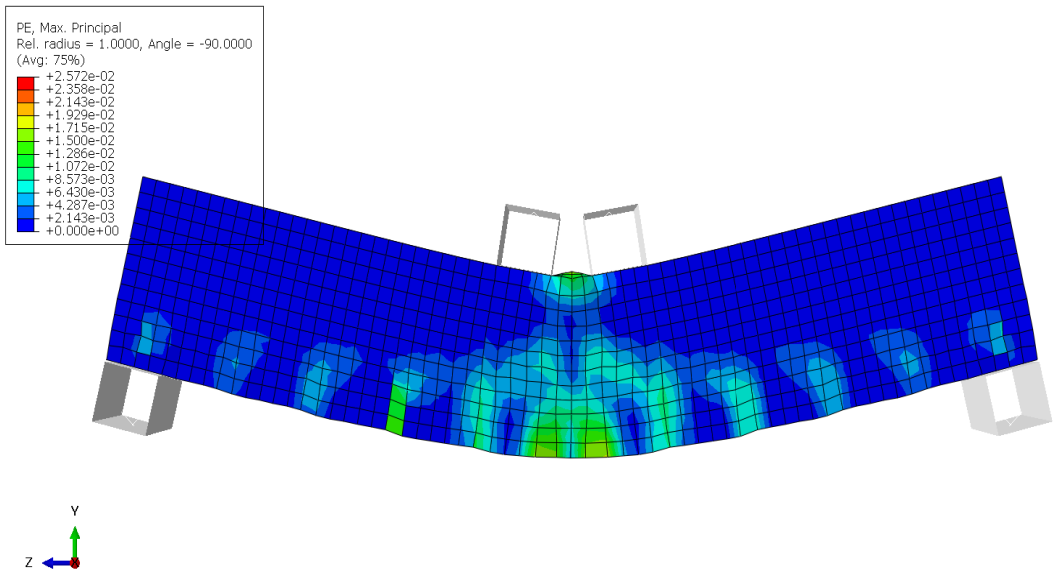

Figure 28. Plastic Strain distribution for Model-I in Abaqus; crack development

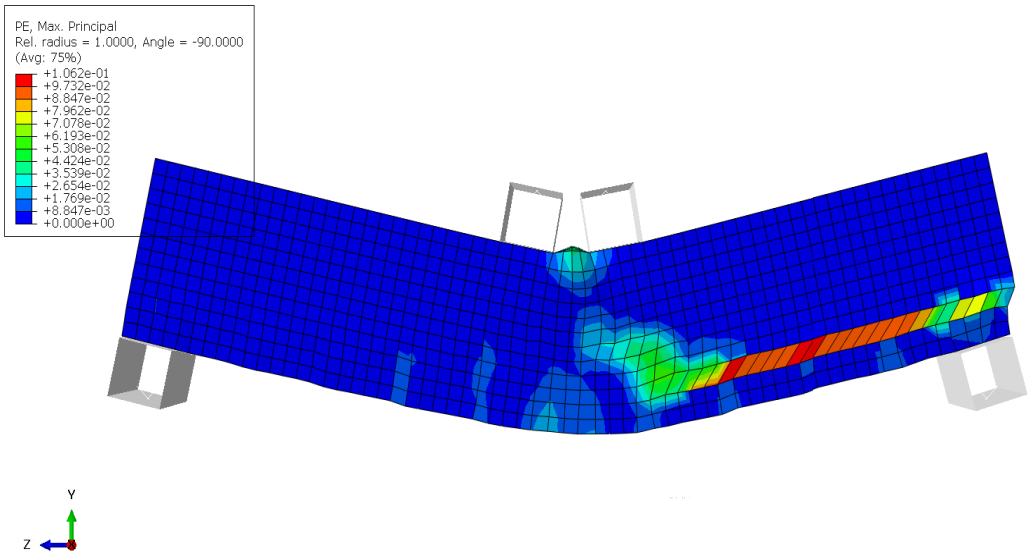

Figure 29. Plastic Strain distribution for Model-I in Abaqus

4.3. Research Model-II

4.3.1 Experimental Benchmark

The second model for the research is based on the research done by Morenon et al. (2019). The experimental data from this research is extensive, and the Beam model dimensions and properties are available for modelling. In this research, the experiment is done on 3.0 m long beams. The effect of ASR is monitored on plain beams, reinforced beams, and heavily reinforced beams. The beam size, dimensions, load locations, and supports, shown in Figure 30.

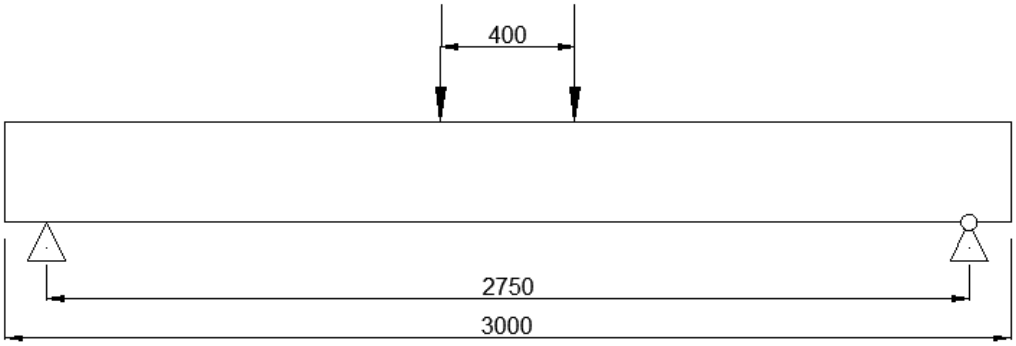

Figure 30. Morenon et al. (2019) experiment beam size, load location & support conditions (all dimensions are in mm)

4.3.2 Model-II Geometry

Research Model-II is based on the same beam as tested and modelled by Morenon et al. (2019).

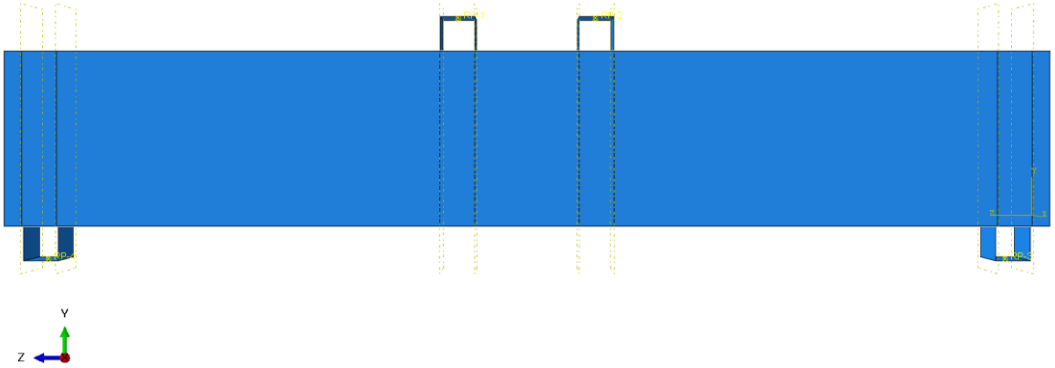

Figure 31. Abaqus Layered beam model, Model-II 2D

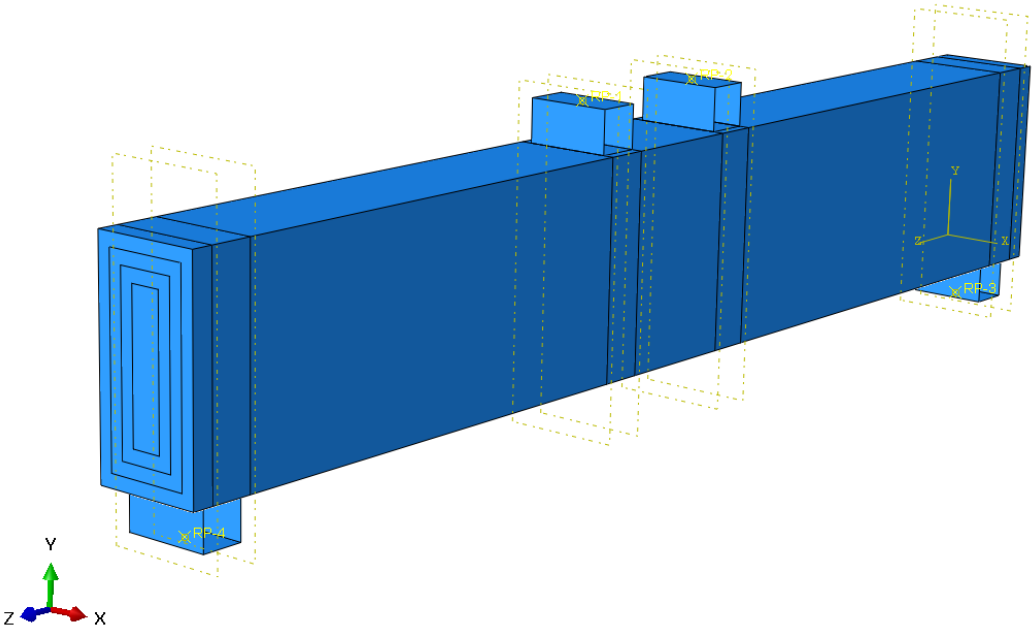

Figure 32. Abaqus Layered beam model, Model-II 3D

The specifics of the beam tested by Morenon et al. (2019) were as follows: the length of the beam is 3.0m, and the cross-section has a dimensional width of 250mm and a height of 500mm. The FEM Model-II setup is with similar loading load & support conditions. The Model-II in Abaqus is shown in Figures 31 & 32. This beam serves as a very suitable model for ASR research, as it is experimented on and modeled by Morenon et al. (2019). So, the Model-II can be compared to the experiments and FEM models, both from the Morenon et al. (2019). Also, the

experimental beam has double layers of reinforcements with stirrups, and the length and dimensions of the beam are ideal for a design. Thus, creating this model will help the ASR research by modelling a realistic doubly reinforced beam and commenting on the ASR effects on a doubly reinforced concrete beam. The layered modelling technique will be validated for a doubly reinforced beam. Furthermore, Morenon et al. (2019) performed tests and created FEM models on both reinforced and unreinforced beams. This is another reason why the comparison will be helpful in validating both reinforced and unreinforced beams.

4.3.3 Model-II Material Properties

Model-II is made up of four models:

a. Model-II No Reinforcement No ASR

b. Model-II No Reinforcement with ASR

c. Model-II with Reinforcement No ASR

d. Model-II with Reinforcement & ASR

For Model-II (a) & (c), without ASR effects, the modulus and plasticity data are the same over the whole segment. Model-II (b) & (d) with ASR, layered modelling approach has been utilized. The material characteristics chosen for all four Model-II with and without ASR effects are displayed in the table below.

Table 6. Material Properties for Model-II No ASR

Model-II No ASR		
Elastic Modulus E	46.4	GPa
Poisson's Ratio	0.2	
Compressive Strength f_{cu}	30	MPa
Tensile Strength ft	2	MPa
Concrete Crushing Stress	10	MPa
Steel Elastic Modulus	180	GPa
Yield Stress f_{sy}	371	MPa

For Model-II (b) & (d), the layered modelling approach has been employed. The models are layered with different moduli for each layer, with the outermost layer having the lowest modulus of 50%. The model is layered in 4 layers. The innermost layer will have a 100% modulus. The four layers of moduli are such: outermost is 50% of modulus, i.e., 23.2GPa, and the second layer is approx. 67% i.e., 31GPa, third layer is approx. 85% i.e., 39.5GPa and the innermost layer is 100% i.e., 46.4GPa. The Modulus properties based on layers are shown in the table below.

Table 7. Material Properties for Model-II ASR

Model-II ASR		
Elastic Modulus E - Layer 1 - Outermost	23.2	GPa
Elastic Modulus E - Layer 2	31	GPa
Elastic Modulus E - Layer 3	39.5	GPa
Elastic Modulus E - Layer 4 - Innermost	46.4	GPa

4.3.4 Load Conditions

Model II is supported in the manner of a simply supported beam with a pinned roller support. Like Model I, the top midpoint is subjected to two predetermined displacements, each of which loads the beam. A support is attached in the direction of the load before the prescribed displacement is attached in the same direction. The reference load, in this instance, is downward-directed. The beam arrangement is shown in Figure 33.

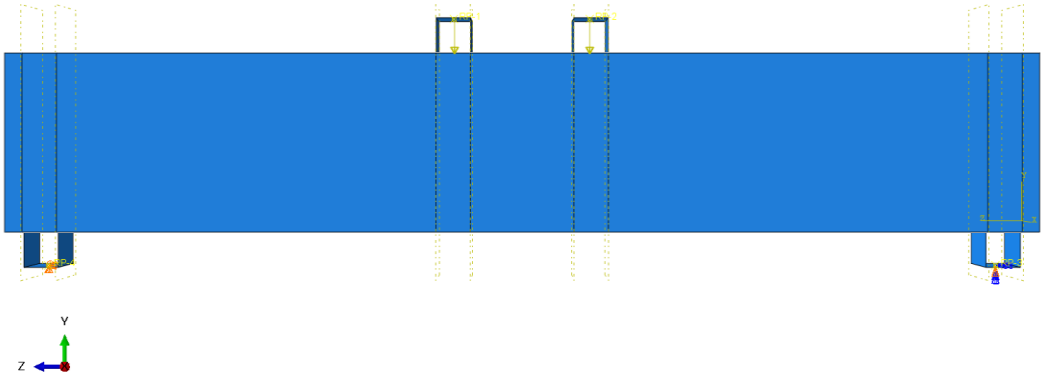

Figure 33. Model-II load & supports arrangement.

4.3.5 Validation of Model-II

The comparison results between unreinforced Model-II and unreinforced beams from Morenon et al. (2019) beams are shown in Figure 34. This comparison between the FEM Model-II and the experimented beams implies that the layered FEM model is able to predict the same behavior and results as the actually experimented beams. Due to this, the layered modelling technique is validated through the validation of the Model-II. The unreinforced plain beams Model-II are compared with the plain beams tested & modeled by Morenon et al. (2019) and have a good agreement. Figure shows two comparisons, a comparison of unaffected & unreinforced plain beams, mentioned as the "Experiment No ASR" and "Model-II No ASR," and the comparison between affected unreinforced plain beams mentioned as "Experiment ASR" and "Model-II ASR".

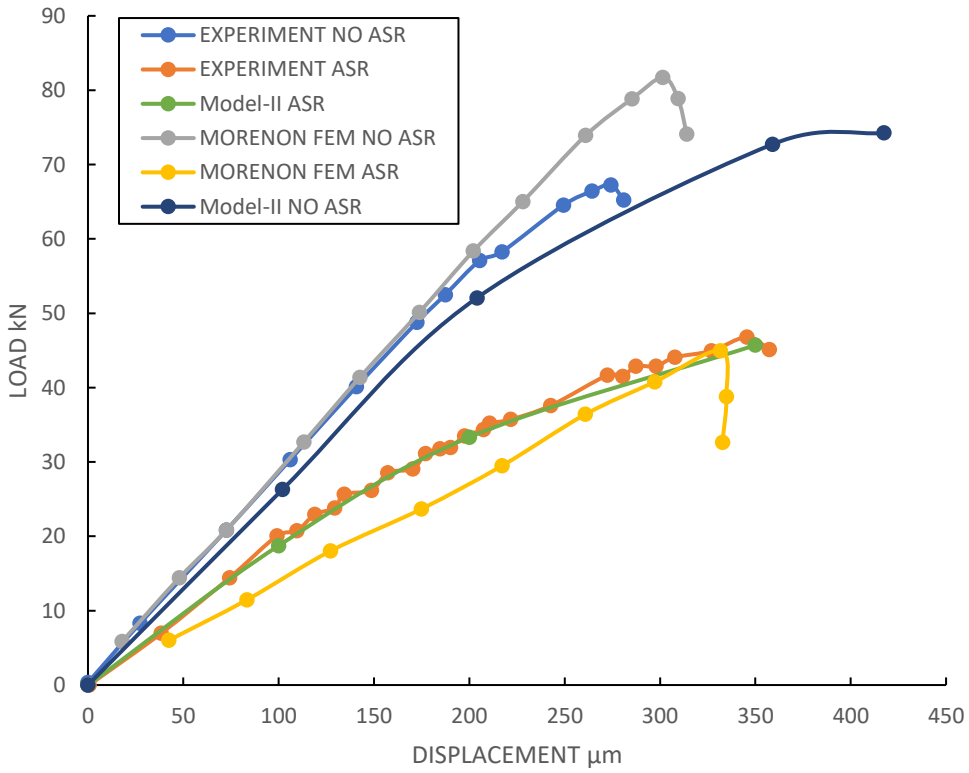

Figure 34. Comparison between the unreinforced plain beams of Model-II and beams tested by Morenon et al. (2019) both with and without ASR effects

In both cases, the values of load-carrying capacities are similar. Morenon et al. (2019) state that the unaffected beam fails at 68 kN compared to 75 kN of Model-II. In the case of ASR-affected beams, Morenon et al. (2019) beam fails at a Load

value of 46 kN, whereas the Model-II fails at a value of 45 kN. This result shows that the Model-II can demonstrate behavior similar to that of the experimented beams. The unreinforced beams possess lower strength than the reinforced beams, so Model-II comparison in Figure above shows that the capacity of Model-II with ASR is reduced by up to 40% compared to the original Model-II No ASR capacity.

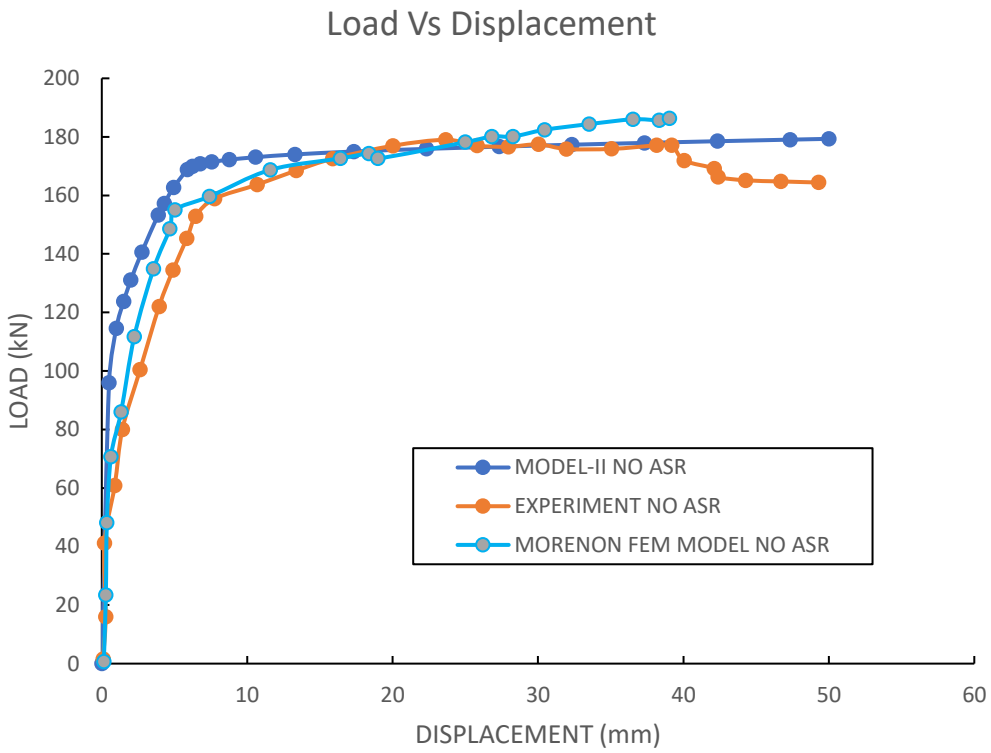

Figure 35. Comparison between the unaffected reinforced beams of Model-II and beams tested by Morenon et al. (2019)

The comparison results between Model-II and Morenon et al. (2019) beams are shown in Figure 35. The unaffected reinforced beam Model-II is compared with the unaffected reinforced beam tested by Morenon et al. (2019) and has a good agreement. The Model-II beam failed at approximately 170 kN, which is quite close to the experimented beam, which failed at 175 kN. The comparison shows that Model-II without ASR is modeled correctly, and so the first step for the reinforced beam model is validated. In the next step, the ASR-affected beam with double reinforcement (top & bottom) is modeled using the data from Table 7. A comparison results shows that the ASR-affected Model-II behavior matches the

ASR experimented beam as shown in Figure 36. Model II fails at a value of 160 kN, which is similar to the tested beam and the FEM model values of 150 kN and 164 kN, respectively. All three Model-II beams can inhibit the flexural behavior similar to the actually experimented beams from Morenon et al. (2019) experiments. The layered modelling technique is able to introduce the ASR effects from the actual experiments. This validation is to confirm the modelling technique and the good agreement between the Model-II, experimented beams, and the FEM models from the experiment, proves the validation.

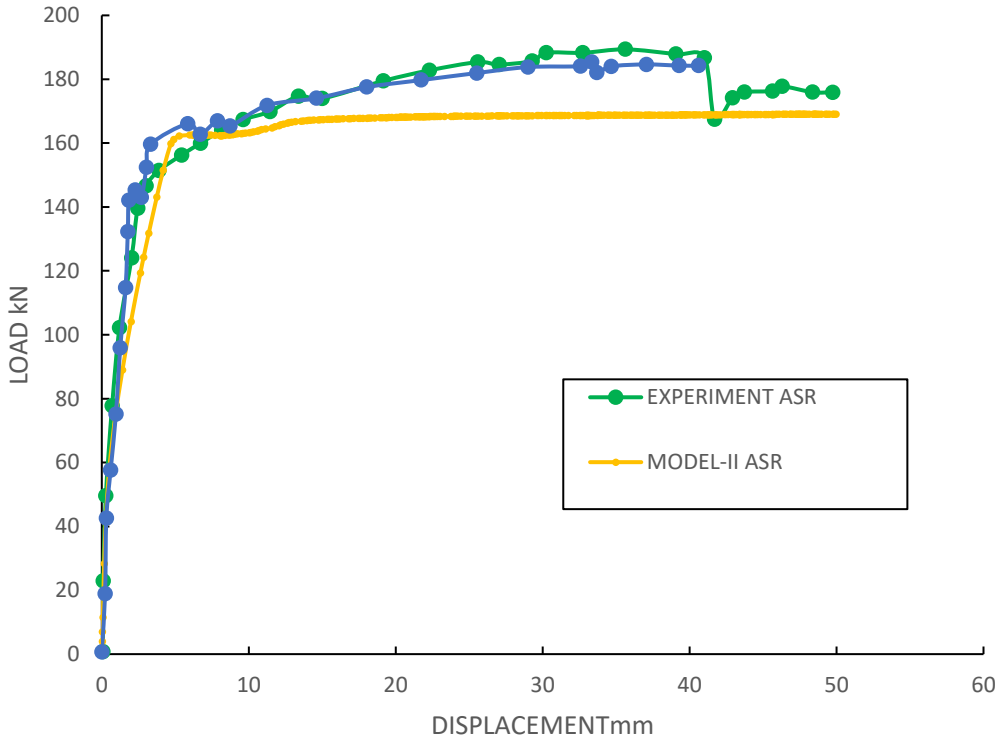

Figure 36. The comparison between unaffected reinforced Morenon et al. (2019) beams, unaffected Model-II & ASR affected Model-II

The Model-II mesh arrangement, as well as the Model-II ASR stress and plastic strain distribution, is shown in Figures 37-40. The mesh arrangement displays the widely used mesh element type, which is hexahedral C3D8R mesh elements used for the concrete beam. This element type has eight nodes. For steel, a 2-node 3D linear truss element type is used. These elements reduce the computational time and effort related to the complexity of mesh arrangement. This mesh type is used

without the reduced integration to avoid convergence error. These mesh element types have lesser chances of element distortion. Moreover, the mesh element size being reasonably small, the analysis is able to capture the stress & strain distribution accurately.

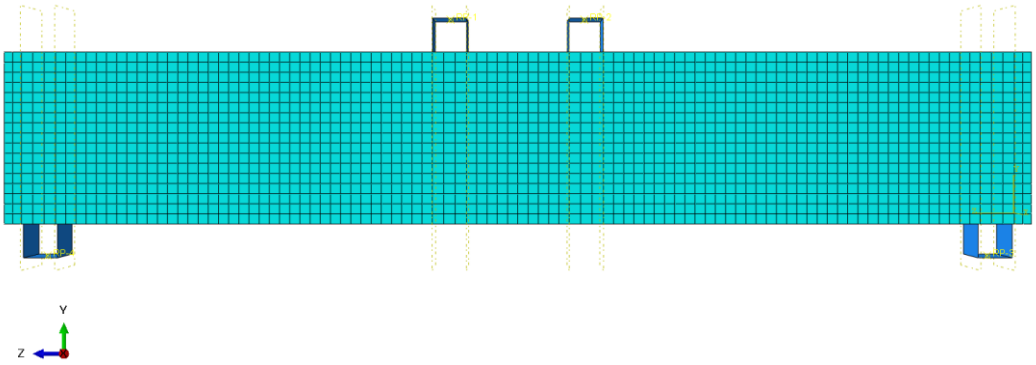

Figure 37. The Mesh arrangement of Model-II

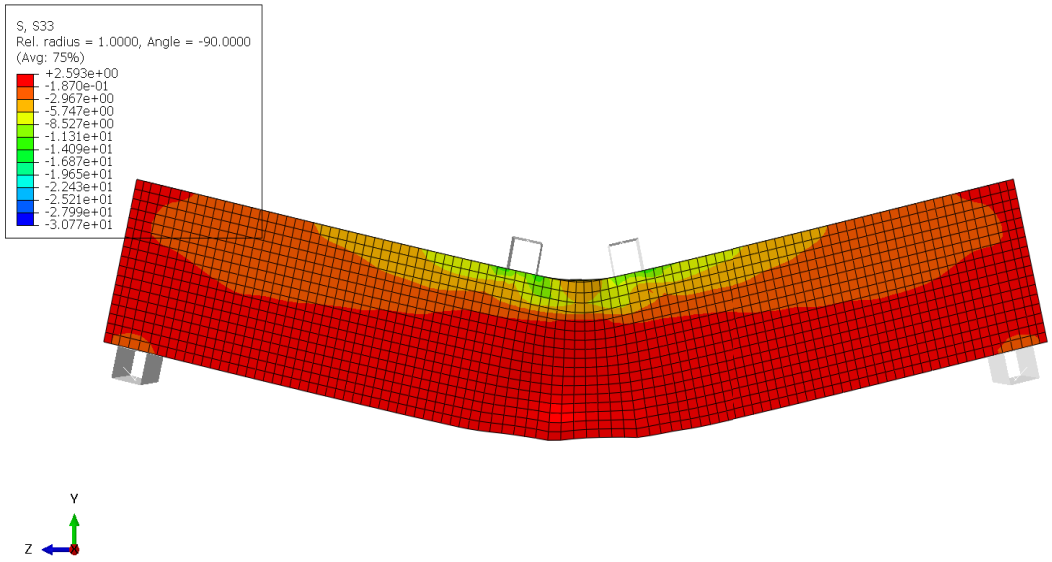

Figure 38. Stress distribution in the longitudinal direction of Model-II with reinforcement

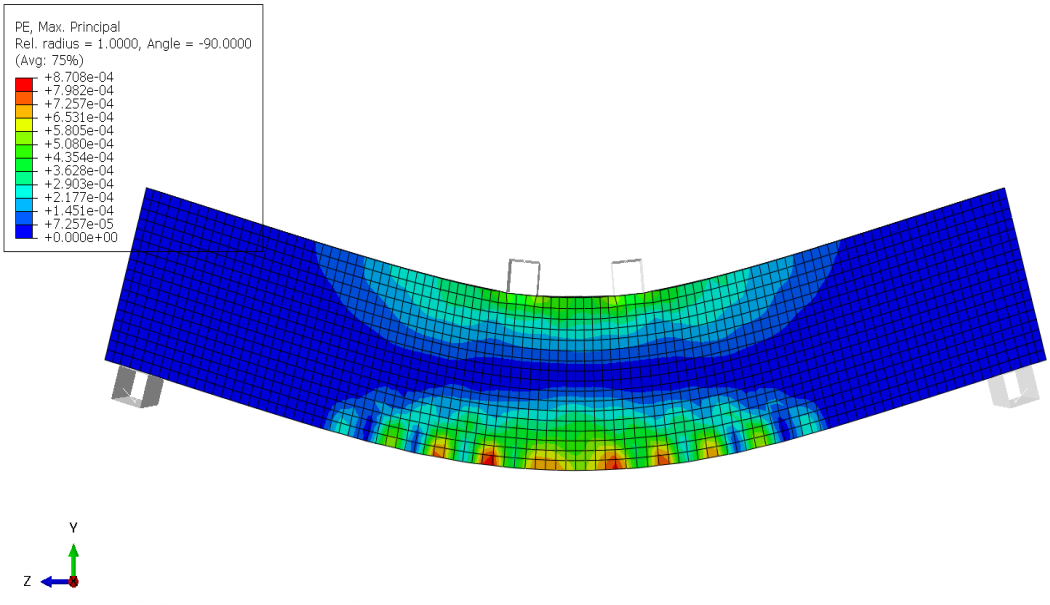

Figure 39. Plastic Strain distribution for Model-I in Abaqus; crack development

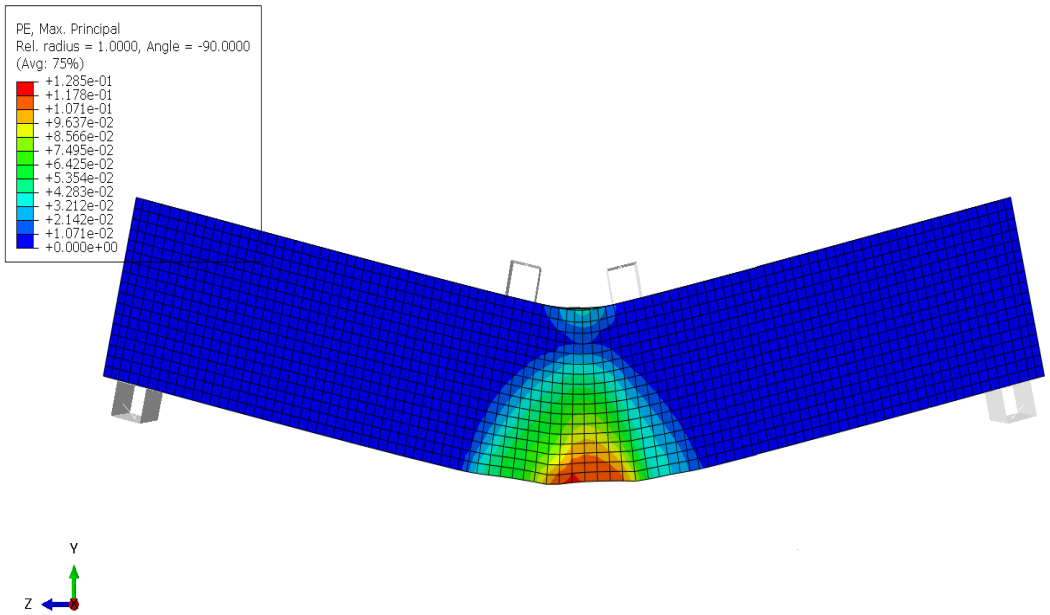

Figure 40. Plastic Strain distribution for Model-I in Abaqus

4.4 Summary

The Layered FEM Model-I and Model-II are developed based on Takahashi et al. (1997) and Morenon et al. (2019) models, are compared with the respective models from the literature then the reduction in Load carrying capacity is discussed.

The model validation seen in this chapter is done in steps for various types of beams. In the first step of the layered model validation process, for singly reinforced beams, the Model-I was developed and compared with the original Takahashi et al. beam. After this, the Model-I with ASR was developed to compare the capacity loss between affected and unaffected beams.

For unreinforced concrete beams, the Model-II based on Morenon et al. (2019) beams was developed, and unreinforced beams with and without ASR effects were compared to Morenon et al. beams. This comparison showed good agreement for both beam models.

Finally, for doubly reinforced with stirrup concrete beams, the Model-II beams with reinforcements were developed and compared individually with Morenon et al. (2019) tested beams and FEM models, and good results were observed for both cases.

The load-bearing capacity is a representation of the structure's utilization and safety. Determining the strength loss caused by ASR is, therefore, crucial. The macro model is helpful in anticipating a reduction in the concrete impacted by ASR's load-bearing capability. The layered models can predict the loss of reduction in the capacity of concrete on the basis of lab data and an assessment of the mechanical properties and deterioration prior to calculating the structural capacity.

CHAPTER 5: FLEXURAL CAPACITY OF ASR AFFECTED STRUCTURES

In this chapter, the theory of the ultimate bearing capacity of the concrete beam is presented, and the example beam model is used for computing flexural strength. To ensure structural safety under the construction loads and service loads, the flexural capacity of the concrete members must be calculated and verified. The ultimate capacity, commonly known as the strength for short, is a section's ultimate flexural strength. Since bending moment and shear force are invariably created in the sections of the most often used flexural members, it is important to confirm the strength of the normal and oblique sections.

The flexural strength in bending is expressed as:

$$M_d \leq M_{uo} \tag{5.1}$$

where Md = design bending moment in the section under consideration.

Mu = flexural strength, also called ultimate flexural capacity of the section.

In the ultimate flexural strength theory, beam's ultimate strength actions are identified by the following beam conditions:

(a) Under-reinforced beams: The area of tensile reinforcement and consequently the steel ratio in under-reinforced beams are such that all of the tensile reinforcement will have yielded before the concrete is crushed.

(b) Balanced beams: Beams where the concrete will be crushed, and the tensile reinforcement will simultaneously yield. Ideal conditions are ones that are in balance.

(c) Over-reinforced beams: The concrete in these heavily reinforced beams is crushed while the steel reinforcement is under stress, causing brittle collapse.

The stress distribution above the Neutral Axis is nearly linear when reinforced concrete beam is subjected to a small moment, as shown in Figure 41b. The stress distribution will gradually become clearly curvilinear when the applied moment is

increased, as shown in Figure 41c, until the outer fibre experiences the maximum stress, the concrete's ultimate strength is reached.

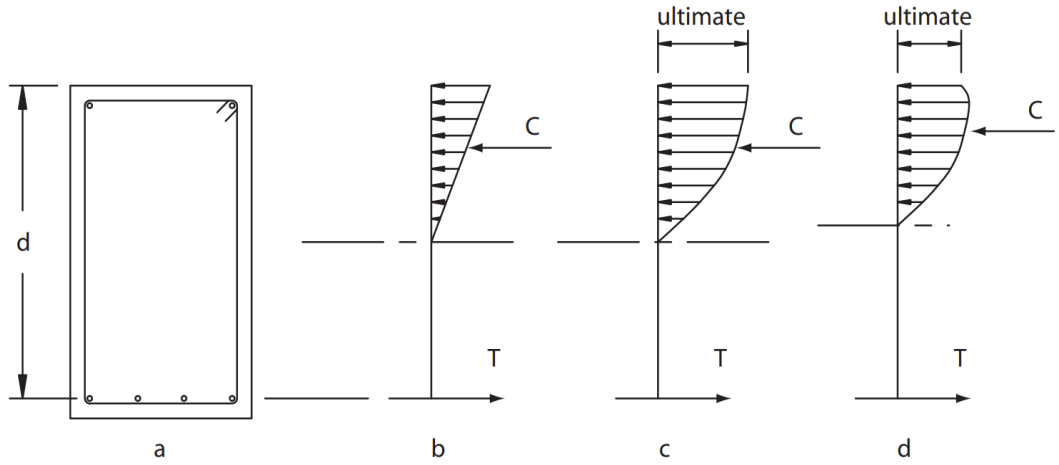

Figure 41 (a-d). The representation of ultimate strength conditions of a beam section

Since the majority of the concrete section is stressed below the concrete's ultimate strength when it is in compression, the concrete section has not yet failed. The selection of the tensile reinforcing area is made so that the yield strength of the steel is reached around the time when the maximum outer concrete stress equals the ultimate strength. The concrete's compressive force, C, balances the reinforcement's tensile force, T, which has achieved its maximum value and is given by T = Ast * fsy. To counteract the moment applied externally, a couple of internal forces called C and T are formed. However, the reinforced concrete part can withstand a greater moment; thus, the concrete has not yet broken. An increase in the internal couple is necessary to raise the external moment, but since the steel is yielding and the tensile force T is not greater than Ast *fsy, the magnitude of the internal forces T and C have reached their maximum. Shifting C to the outer fiber increases the internal lever arm while decreasing the depth of the neutral axis. In order to maintain equilibrium, increased concrete stresses are required if the depth of the neutral axis is decreased because less concrete will be compressed. The final stress conditions will be applied to a larger area of concrete, eventually causing failure and Figure 41 d shows the stress distribution at failure.

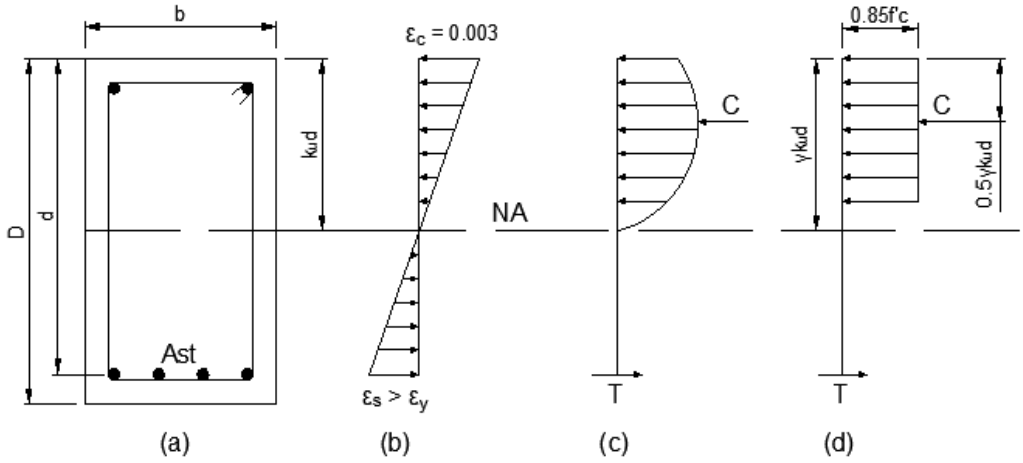

Figure 42 (a-d). The representation of a beam section at ultimate strength conditions

The diagram with a maximum concrete strain of c = 0.003, as previously defined, is shown in Figure 42b when an under-reinforced concrete beam is considered to be on the verge of failure. The actual stress diagram, shown in Figure 42 c, results in a compressive force C balancing the tensile force T and a tensile force T = Ast * fsy acting on the beam. Assessing the lever arm between C and T will be required in order to establish the internal moment of resistance. It becomes clear that it is challenging to find force C's location with respect to the neutral axis. Numerous scholars have provided descriptions of the compressive stress distribution known as the stress block. Based on the above-presented theory of the ultimate strength of concrete beam in flexure, in the following sections, computation of ultimate flexural strength is presented for Model-I and Model-II beams.

5.1 Ultimate Moment Capacity M_{uo}

The coupling of internal forces C and T gives the ultimate moment capacity is shown in Figure 42.

Following expression is obtained by considering moment at C,

$$M_{uo} = T(d - 0.5\gamma k_u d) \quad (5.2)$$

$$= A_{st}\,(f_{sy})\,(d - 0.5\gamma k_u d) \quad (5.3)$$

$$= A_{st}\,(f_{sy})\,d(1 - 0.5\gamma k_u) \quad (5.4)$$

5.2 Ultimate Moment Capacity M_{uo} for Takahashi et al. (1997)

The ultimate moment capacity for the beam section of Takahashi et al. (1997) can be computed based on the section details, the reinforcement details and Ultimate moment theory. Following data can be depicted from the literature Erkmen et al. (2017);

Section details: width b = 0.2 m & depth D = 0.3 m, d = 0.237 m, cover is assumed 50mm.

Compressive strength = 40.3 MPa, Young's Modulus E = 44.5GPa, fsy = 500 MPa
Area of Steel reinforcement = 1100mm^2

For a given area of reinforcement, following equations 5.5 & 5.6 can be employed to find the ultimate moment capacity of the section:

$$\mathrm{Muo} = \mathrm{f'c}\,(\mathrm{z})\left(1-\frac{\mathrm{z}}{1.7}\right)\mathrm{b}\,\mathrm{d}^2 \tag{5.5}$$

$$\mathrm{z} = \mathrm{p}\left(\frac{\mathrm{fsy}}{\mathrm{f'c}}\right) \tag{5.6}$$

Since, f'c ≥ 28 MPa, γ = 0.85 - 0.007(f 'c – 28) as per AS 3600 (clause 8.1.2.2)

For f'c ≥ 28 MPa, γ ≥ 0.65, and so as per calculation γ = 0.7639 ≈ 0.77

Steel ratio p can be calculated as follows:

$$\mathrm{p} = \frac{\mathrm{A_{St}}}{\mathrm{bd}} = \frac{1100}{200 * 237} = 0.0232$$

Following can be deduced by rearranging the Equations 5.2, 5.3 & 5.4;

$$\mathrm{ku} = \left(\frac{1}{0.85\gamma}\right)\left(\frac{\mathrm{Ast}}{\mathrm{bd}}\right)\left(\frac{\mathrm{fsy}}{\mathrm{f'c}}\right) \tag{5.7}$$

$$\mathrm{ku} = 0.4399$$

Assuming Ku = 0.4 maximum as per AS 3600.2018 (clause 8.1.3).

Depth of neutral axis = k_u d = 0.4 x 237 = 94.8mm

From equation 5.6;

$z = p\left(\frac{fsy}{f'c}\right) = 0.0232\left(\frac{500}{40.3}\right) = 0.2878 \approx 0.288$

As per equation 5.7, the ultimate moment capacity of the Takahashi et al. (1997) beam becomes as follows:

$$\text{Muo} = \text{f'c}\,(\text{z})\left(1-\frac{\text{z}}{1.7}\right)\text{b}\,\text{d}^2 = 40.3\,(0.288)\left(1-\frac{0.288}{1.7}\right)*200*237^2*10^{-6}$$

$$\text{Muo} = 108.295 \approx 110\ \text{kNm}$$

The Takahashi et al. (1997) beam has the bottom reinforcement only and so the moment capacity value may be lower than the actual design case of a beam design.

5.3 Ultimate Moment Capacity M_{uo} for FEM Model-I based on Takahashi et al. (1997)

In the following section, the ultimate moment scenario for layered model for the Takahashi et al. (1997) is computed, to obtain results for ultimate flexural strength for ASR affected concrete beam section and to compare the ultimate capacity with the conventional unaffected Beam Section as done previously. The layered section of Takahashi et al. (1997) i.e., Model-I can be presented as show in Figure 43.

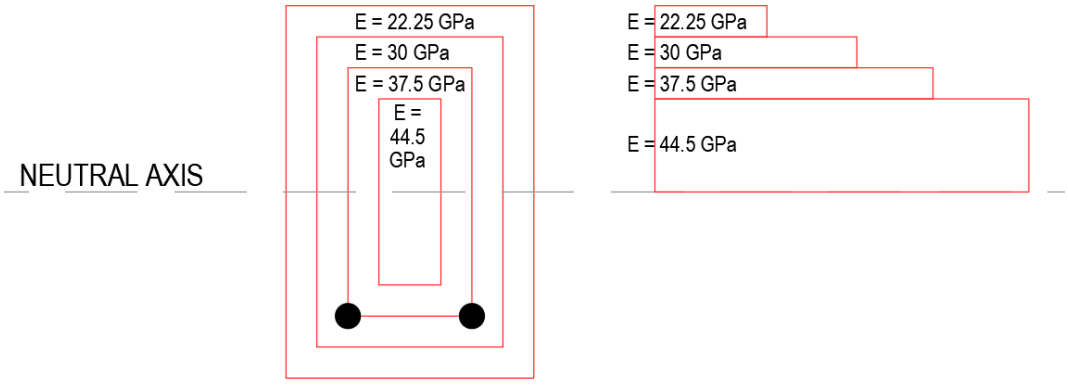

Figure 43. Equilibrium Rectangular Stress Block scenario at ultimate strength conditions for Model-I

The application of moduli within the beam cross-section, with the outermost layer having the loss of up to 50% and the innermost layer having the original 100% modulus of elasticity is shown in Figure 43.

As the moduli varies, the corresponding concrete compressive strength also changes, and the so based on the Equilibrium Rectangular Stress Block theory at

ultimate strength conditions, for calculating Ultimate flexural capacity of a beam section, changes as shown in Figure 44.

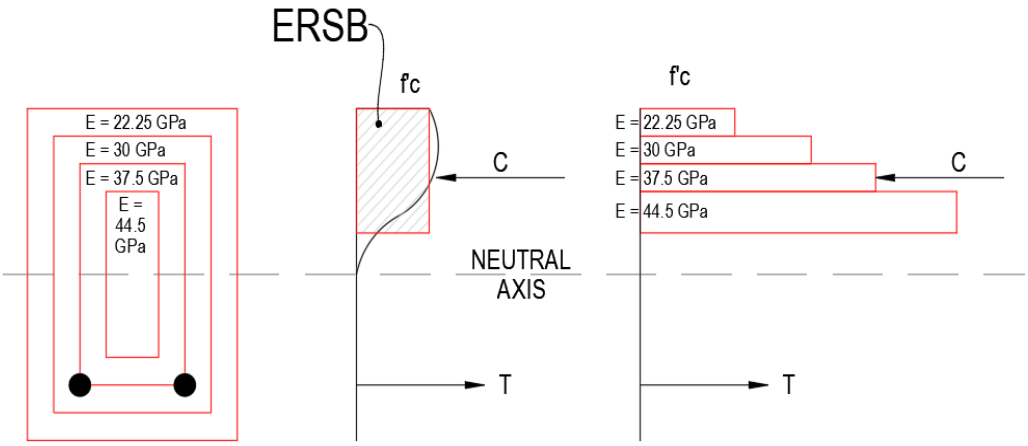

Figure 44. The representation of a layered beam model section at ultimate strength conditions for Model-I

The layered moduli section of the Model-I beam can be used for designing the beam similar to the design of conventional RC beam. The calculation of the ultimate strength can be used for commenting on the actual drop in the strength of a beam affected by ASR.

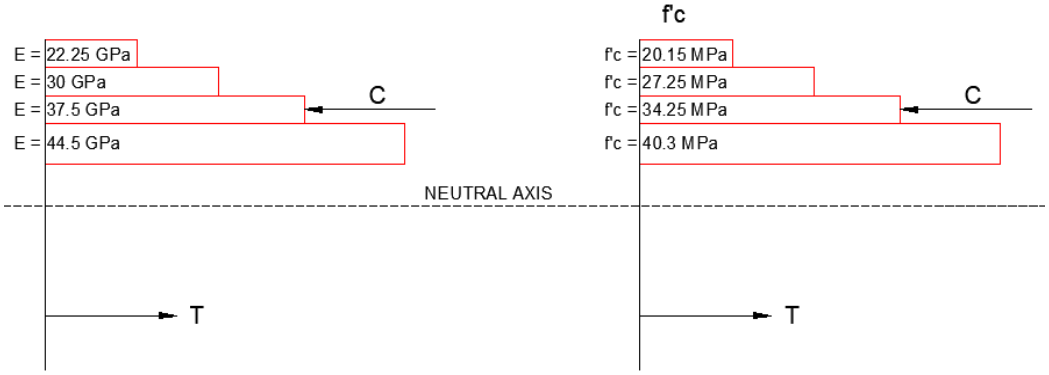

Figure 45. The layered beam Model-I; elastic modulus and compressive strength

The ultimate moment capacity for the beam section of Model-I can be computed based on the section details, the reinforcement details and Ultimate moment theory. Following data is depicted from the literature Erkmen et al. (2017):

Section details: width b = 0.2 m & depth D = 0.3 m, d = 0.237 m, assuming 50mm cover. Yield stress of steel f_{sy} = 500 MPa, area of steel reinforcement = 1100mm^2.

The change in the ASR affected section will be in the Modulus of layers within the section and their corresponding compressive strengths.

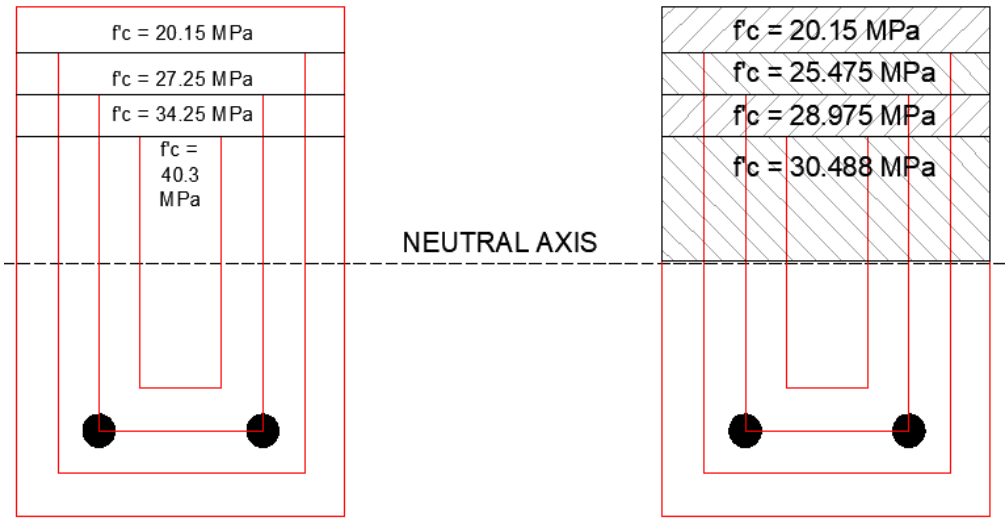

Figure 46 (a) & (b). The layered beam Model-I; compressive strength

The compressive strength f'c can be computed similar to the modulus of various layers. Considering the percentage drop in the modulus for various layers, the compressive strength is computed accordingly, such as different compressive strength for different layers, as presented in the figure above.

For example, in Figure 46 (a), the compressive strength f'c for the top layer is 20.15MPa, the strength for second layer will be 27.25Mpa times the percentage area + 20.15MPa times the percentage area. The final averaged values of f'c are shown in in Figure 46 (b).

Using area of the various stress intensity of the beam section, an average value of compressive strength can be computed for the section as shown in the Figure 47.

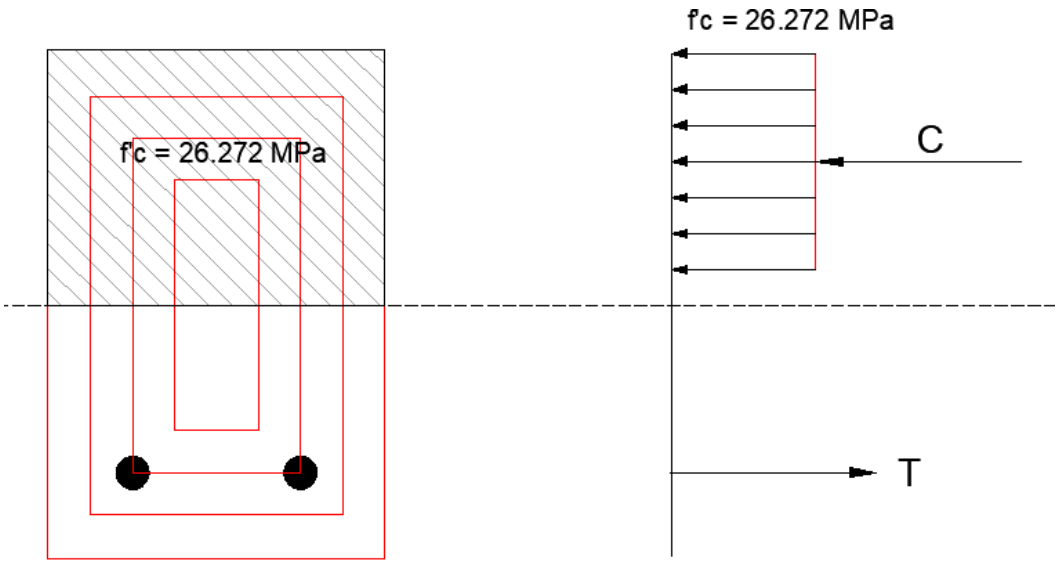

Figure 47. The layered beam Model-I; average compressive strength

Considering the value of compressive strength, the ultimate moment capacity can be computed.

Since, f'c < 28 MPa, γ = 0.85 as per AS3600 (clause 8.1.2.2)

Steel ratio p can be calculated as follows:

$$p = \frac{A_{St}}{bd} = \frac{1100}{200 * 237} = 0.0232$$

Following can be deduced by rearranging the Equations 5.2, 5.3 & 5.4;

$$ku = \left(\frac{1}{0.85\gamma}\right)\left(\frac{Ast}{bd}\right)\left(\frac{fsy}{f'c}\right) = \left(\frac{1}{0.85 * 0.85}\right)0.0232\left(\frac{500}{26.272}\right) = 0.611$$

Assuming Ku = 0.4 maximum as per AS3600 (clause 8.1.3).

Depth of neutral axis = k_u d = 0.4 x 237 = 94.8mm

From equation 5.6;

$$z = p\frac{f_{sy}}{f'_c} = 0.0232\frac{500}{26.272}$$

= 0.4415 ≈ 0.4

As per equation 5.5, the ultimate moment capacity of the Takahashi et al. (1997) beam becomes as follows:

$$\text{Muo} = f'c\,(z)\left(1-\frac{z}{1.7}\right) b\,d^2$$

$$= 26.272 * 0.442 * 1-\frac{0{\cdot}442}{1{\cdot}7} * 200 * 237^2 * 10^{-6}$$

$$\text{Muo} = 96.53 \approx 97 \text{ kNm}$$

The computation ultimate strength capacity of the Takahashi et al. (1997) beam and the Model-I shows the loss in flexural strength. The loss of at least 11% in the ultimate flexural capacity is seen in this computation. The beam, however, is singly reinforced considering bottom reinforcement only, however, for a doubly reinforced beam the strength capacity and the loss in capacity needs to be computed.

5.4 Ultimate Moment Capacity M_{uo} for Morenon et al. (2019)

For the Morenon et al. (2019) beam, the experiment had considered two layers of reinforcement as well as the stirrups along the length of the beam. It is an ideal beam scenario in the practical design work, however, the area of steel in compression is as same as the area of steel in tension, so this model can be computed as a singly reinforced beam. The bars and stirrup sizes are also considered fairly. Length of the beam is 3m.

For computing the ultimate moment capacity, following data can be obtained from the literature.

Section details: width b = 0.25 m & depth D = 0.5 m,

d = D – 50 cover – R10 stirrup – 0.5 x N16 bar = 432mm

Compressive strength = 38.3 MPa, Young's Modulus E = 46.4GPa, fsy = 500 MPa
Area of Steel reinforcement = 402mm^2

Since, f'c ≥ 28 MPa, $\gamma = 0.85 - 0.007(f'c - 28)$ as per AS3600 (clause 8.1.2.2)

For f'c ≥ 28 MPa, $\gamma \geq 0.65$, and so as per calculation $\gamma = 0.7779 \approx 0.78$

Maximum steel ratio p can be calculated from equation (5.8) as follows:

$$\text{pmax} = 0.34\ \gamma\ \left(\frac{f'c}{fsy}\right) \qquad (5.8)$$

$$= 0.34 * 0.78 * \left(\frac{38.3}{500}\right)$$

$$p = 0.0203$$

Finding $K_u d$ by rearranging the Equations 5.2, 5.3 & 5.4;

$$ku = \left(\frac{1}{0.85\gamma}\right)\left(\frac{Ast}{bd}\right)\left(\frac{fsy}{f'c}\right)$$

$$ku = \left(\frac{1}{0.85 * 0.78}\right)0.0203\left(\frac{500}{38.3}\right)$$

$$ku = 0.399$$

Assuming Ku = 0.4 maximum as per AS3600 (clause 8.1.3).

Depth of neutral axis = k_u d = 0.4 x 432 = 172.8mm

From equation 5.6;

$$z = p\left(\frac{fsy}{f'c}\right) = 0.0203\left(\frac{500}{38.3}\right) = 0.265$$

As per equation 5.5, the ultimate moment capacity of the Morenon et al. (2019) beam becomes as follows:

$$Muo = f'c\,(z)\left(1 - \frac{z}{1.7}\right) b\,d^2 = 38.3\,(0.265)\left(1 - \frac{0.265}{1.7}\right) * 250 * 432^2 * 10^{-6}$$

$$Muo = 399.71 \approx 400\ kNm$$

5.5 Ultimate Moment Capacity M_{uo} for FEM Model-II based on Morenon et al. (2019)

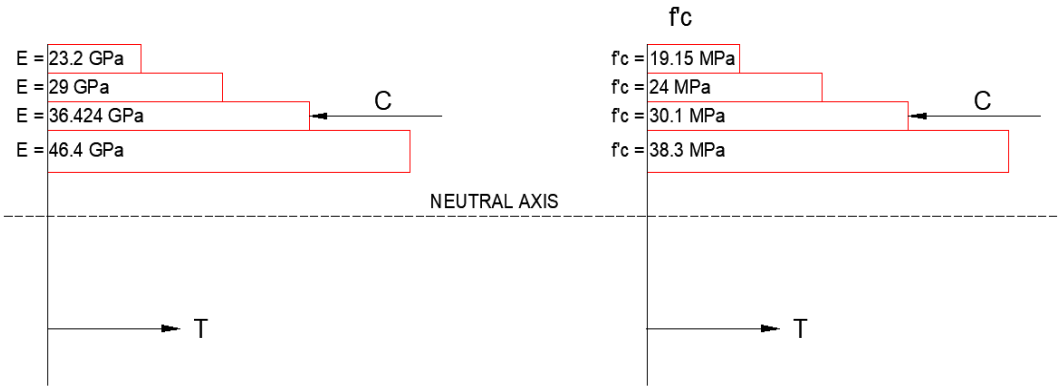

Figure 48. The layered beam Model-II; elastic modulus and compressive strength

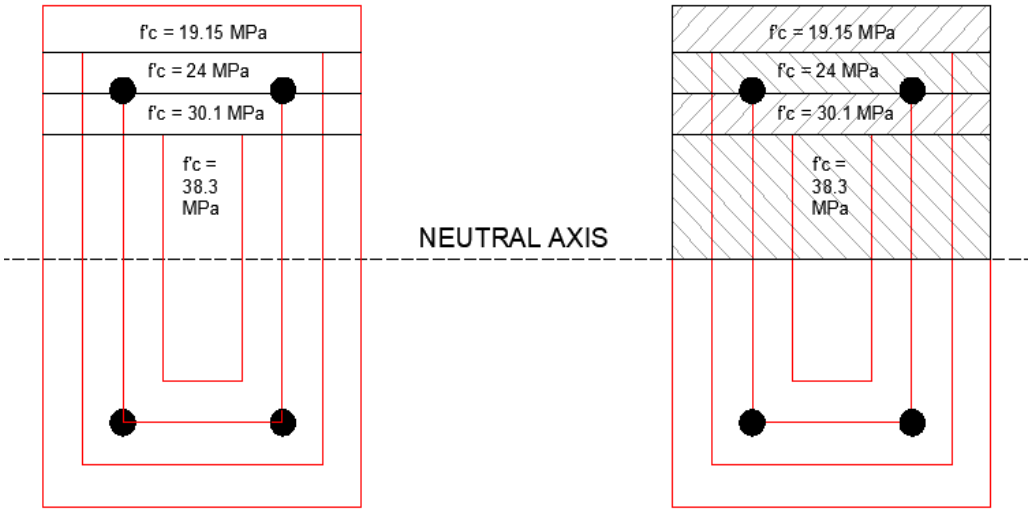

Figure 49. The layered beam Model-II; compressive strength

The layered moduli section of the Model-II beam can be used for designing the beam similar to the design of conventional RC beam. By computing the value of compressive strength, the ultimate moment capacity can be computed.

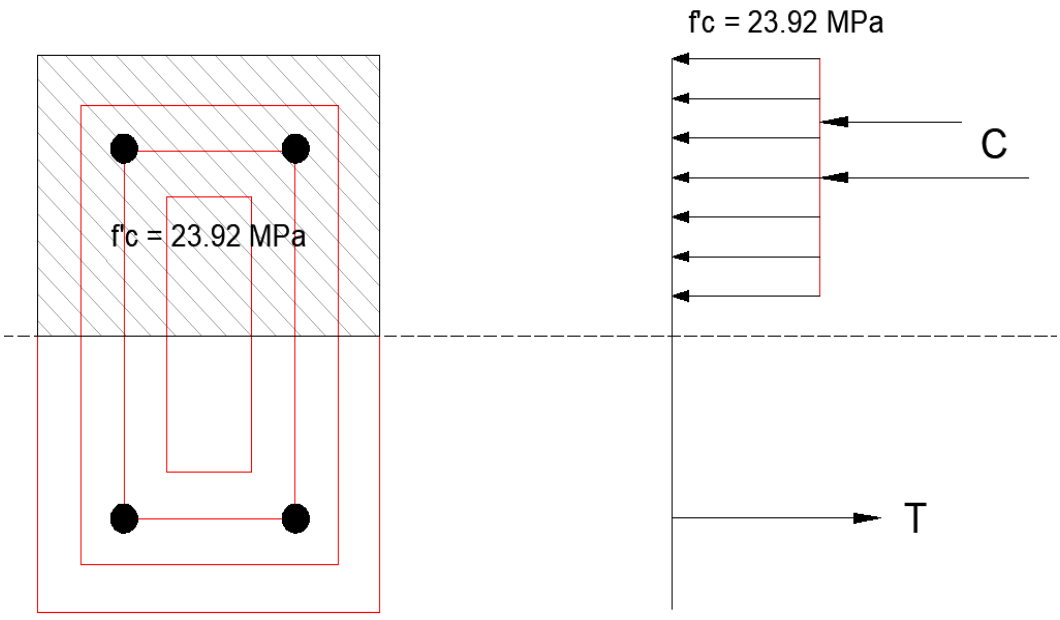

Figure 50. The layered beam Model-II; average compressive strength

Since, f'c < 28 MPa, γ = 0.85 as per AS3600 (clause 8.1.2.2)

Maximum steel ratio p can be calculated from equation (5.8) as follows:

$$\text{pmax} = 0.34\ \gamma \left(\frac{\text{f'c}}{\text{fsy}}\right)$$

$$\text{p} = 0.34 * 0.85 * \left(\frac{23.92}{500}\right)$$

$$\text{p} = 0.0138$$

Following can be deduced by rearranging the Equations 5.2, 5.3 & 5.4;

$$\text{ku} = \left(\frac{1}{0.85\gamma}\right)\left(\frac{\text{Ast}}{\text{bd}}\right)\left(\frac{\text{fsy}}{\text{f'c}}\right)$$

$$\text{ku} = \left(\frac{1}{0.85 * 0.85}\right) 0.0138 \left(\frac{500}{23.92}\right)$$

$$\text{ku} = 0.399$$

Assuming Ku = 0.4 maximum as per AS3600 (clause 8.1.3).

Depth of neutral axis = k_u d = 0.4 x 432 = 172.8mm

From equation 5.6;

$$\text{z} = \text{p}\left(\frac{\text{fsy}}{\text{f'c}}\right) = 0.0203\left(\frac{500}{23.92}\right) = 0.424 \approx 0.424$$

As per equation 5.5, the ultimate moment capacity of the Model-II beam becomes as follows:

$$\text{Muo} = \text{f'c}\ (\text{z})\left(1 - \frac{\text{z}}{1.7}\right) \text{b}\ \text{d}^2 = 23.92\ (0.424)\left(1 - \frac{0.424}{1.7}\right) * 250 * 432^2 * 10^{-6}$$

$$\text{Muo} = 355.17 \approx 356\ \text{kNm}$$

The computation ultimate strength capacity of the Morenon et al. (2019) beam and the Model-II shows the loss in Ultimate flexural strength. The loss of at least 11% in the ultimate flexural capacity is seen in this computation, similar, to Takahashi et al. (1997) and Model-I scenario.

5.6 Summary

This chapter showed the capacity computation based on the layered model approach. For both the beams, Takahashi et al. (1997) and Morenon et al. (2019), the ultimate flexural capacity is observed to have reduced due to ASR-related varying moduli layers. The loss in strength also matches the data presented in Chapter 2. Kobayashi (1988) and Inoue (1989) both commented, based on

experiments, that a drop of approximately 10% is observed in the ASR-affected beams, which is similar to the 11% drop in the computation seen in this chapter. This suggests that the layered modelling approach is applicable to forecast the capacity loss in beams affected by ASR.

CHAPTER 6: CONCLUSION & RECOMMENDATIONS

6.1 Conclusions

The main aim of this study was to present a novel modelling technique for assessing the ultimate flexural capacity of reinforced concrete structures impacted by ASR. First, the theory was developed using a strong literature review. Then, the finite element numerical models were put forth to validate the theory based on observed effects in laboratory/ experimental studies. To further validate the loss in flexural strength capacity of reinforced concrete beams due to ASR, the ultimate flexural capacities of the beams were computed based on Concrete Standard AS3600. Based on laboratory data and an evaluation of the mechanical characteristics deterioration before determining the structural capacity, the proposed models were able to validate a layered modelling approach.

Three main chapters, i.e., 3, 4 & 5, led to the following conclusions.

6.2 Reduction of mechanical properties due to ASR in layers

Most studies on the topic demonstrate that the compressive strength & mostly, the modulus of elasticity saw a significant reduction in Chapter 3. However, the reported experimental data revealed substantial variability in the loss of elasticity modulus in a differential manner. The development of the layered model approach is a useful way of depicting the loss of properties within the section by modelling in layers. When it comes to cracks and loss in strength, numerous experimental literature have shown reductions in strength and demonstrate the formation of larger cracks at the outermost surface compared to the innermost, thus giving the idea of the layered model.

6.3 Numerical modelling of beams affected by ASR and comparison with experimental data.

In Chapter 4, numerical modelling predicts the behavior of ASR-affected beams. The comparison of the models with the existing research proves the suitability of the layered model approach. The concrete damaged plasticity model was used to develop the finite element-based numerical model in the commercial FEA

software ABAQUS. By considering the effects of crack formation that are evident in ASR-affected structures, the numerical models were proposed.

Practicing engineers can utilise the finding in this study to estimate the loss in strength at ultimate conditions. The model technique developed in this study and the strength computation presented in Chapter 5 is very useful for computing strength loss in ASR affected beam.

6.4 Discussion of Design & Capacity Reduction

- The model in this research serves as a stepping stone for the Engineering design approach. The model has layered moduli, which reflects the actual impact of ASR on a concrete element. This information is useful in designing a concrete beam that is affected by ASR. The various moduli from the layered model can help estimate the flexural strength of the beam, and thus, the design capacity can be commented upon when the beam acts under various load conditions. The variance in the moduli can reflect that the design approach of an ASR-affected beam can be different from that of a conventional reinforced concrete beam. This can be seen in Chapter 5 in the computation part, where the reduction in the Ultimate Moment Capacity is evident, and loss is considerable.

6.5 Recommendations for future studies

- Based on the findings of this thesis, a number of topics are suggested for further study to advance our understanding of the diagnosis of existing ASR-damaged structures through layered modelling techniques. Following are some recommendations with further details:
- Gather more experimental data: Although the novel layered modelling approach can shed light on how to incorporate the change in mechanical properties in an affected beam model, more experimental data on the properties of concrete and crack formation within the domain affected by ASR are desired to increase model accuracy and improve the evaluation of the effects of influencing factors. Particularly, incorporating expansion

data in the model, more data is needed to evaluate ASR-affected concrete in the field from the laboratory and samples/members from the field.

- Investigate additional factors and phenomena: Future study should focus on the problems such as loss in shear strength, temperature effects, modelling of columns and slabs, especially for simulating prestressed concrete members. It is also necessary to investigate the bond slip behaviour of steel in ASR affected reinforced concrete, as well as how it affects structural capacity.
- Studies can include steel corrosion. Due to larger cracks and deterioration, the durability of the concrete is reduced due to higher chances of steel corrosion. This topic can also be included in the future studies.

REFERENCES

Ahmed, T. B. (1999). Effect of alkali-silica reaction on tensile bond strength of reinforcement in concrete tested under static and fatigue loading. *Materials Journal, vol. 96, no. 4*, pp. 419-428.

Ahmed, T. B.-T. (2003). The effect of alkali reactivity on the mechanical properties of concrete. *Construction and Building Materials, 17*(2), pp. 123-144.

Ben Haha, M. (2006). *Mechanical effects of alkali silica reaction in concrete studied by SEM-image analysis." Ph.D. thesis.* Lausanne, Switzerland: École Polytechnique Fèdèrale de Lausanne, Lausanne, Switzerland.

Charlwood R.G., S. S. (n.d.). A review of alkali aggregate reactions in hydroelectric plants and dams. . *Proceedings of the International Conference of Alkali-Aggregate Reactions in Hydroelectric Plants and Dams, Fredericton, Canada, vol. 129.*

Courtier, R. (1990). The assessment of ASR-affected structures. *Cement and Concrete composites, vol. 12, no. 3*, pp. 191-201.

Dunant, C. (2009). *Experimental and modelling study of the alkali-silica-reaction in concrete.* PhD thesis. École Polytechnique Fédérale de Lausanne, Switzerland.

Erkmen R.E., G. N. (2017). Elasto-plastic damage modelling of beams and columns with mechanical degradation. *Computers and Concrete*, Vol. 19, No. 3, pp. 315-323.

Esposito, R. A. (2016). Influence of the alkali-silica reaction on the mechanical degradation of concrete. *Journal of Materials in Civil Engineering, vol. 28, no. 6*, p. 04016007.

Garcia-Diaz, E. R. (2006). Mechanism of damage for the alkali–silica reaction. *Cement and Concrete Research, vol. 36, no. 2*, pp. 395-400.

Giaccio, G., Zerbino, R., Ponce, J., & Batic, O. (2008). Mechanical behavior of concretes damaged by alkali-silica reaction. *Cement and Concrete Research, vol. 38, no. 7*, pp. 993-1004.

Giannini, E. &. (2012). Stiffness damage and mechanical testing of cores specimens for the evaluation of structures affected by ASR. *14th International Conference on Alkali Aggregate Reaction (ICAAR14).* Austin, Texas.

Giorla, A. (2013). *Modelling of alkali-silica reaction under multi-axial load.* PhD thesis. École Polytechnique Fédérale de Lausanne, Switzerland.

Gowripalan, N. C. (2021). Comparison of the effect of ASR deterioration on the load carrying capacity of concrete structural elements in accelerated laboratory tests and in the field. Lisboa: ICAAR.

Hafezolghorani, M. H. (2017). Simplified Damage Plasticity Model for Concrete. *Structural Engineering International*, pp. 68-78.

Hiroi, Y. Y. (2016). Experimental and analytical studies on flexural behaviour of post-tensioned concrete beam specimen deteriorated by alkali-silica reaction (ASR). *15th International Conference on Alkali-Aggregate Reaction, Sao Paulo Brazil*, (pp. 03-07).

Hobbs, D. (1988). *Alkali-silica reaction in concrete.* Thomas Telford Ltd, London.

Inoue, S. F. (1989). Structural behaviors of reinforced concrete beams affected by alkali-silica reaction. *8th International Conference on Alkali-Aggregate Reaction, ICAAR, Kyoto, Japan*, pp. 727–732.

ISE. (1992). *Structural effects of alkali-silica reaction. Technical guidance on the appraisal of existing structures.* London, United Kingdom: SETO Ltd.

Kagimoto, H. Y. (2014). ASR expansion, expansive pressure and cracking in concrete prisms under various degrees of restraint. *Cement and Concrete Research, vol. 59*, pp. 1-15.

Kawamura, M. (2007). Estimation of critical free expansions related to surface cracking in ASR-affected concretes. *Cement & Concrete Composites, vol. 29, no. 4*, pp. 324-329.

Kobayashi, K. I. (1988). Alkali aggregate reaction in prestressed concrete beams. *International Journal of Cement Composites and Lightweight Concrete, vol. 10, no. 4*, pp. 233-240.

Kongshaug SS, O. O. (2020). Experimental investigation of ASR-affected concrete -The influence of uniaxial loading on the evolution of mechanical properties, expansion and damage indices. *Construction and Building Materials, 245*, 7.

Kubo, Y. &. (2012). Effect of Reactive Aggregate on Mechanical Properties of Concrete Affected by Alkali–Silica Reaction. *14th International Conference on Alkali–Aggregate Reaction.*

Larive, C. (1998). *Apports combinès de l expèrimentation et de la modèlesllisation á la comprehènsion de l'alcali-rèaction et de ses effets mècaniques.* Paris, France: PhD thesis. Èncole Nationale des Ponts et Chaussèes.

Mohammed, T. H. (2003). Relation between Strain on Surface and Strain over Embedded Steel Bars in ASR Affected Concrete Members. *Journal of Advanced Concrete Technology*, vol. 1, no. 1, pp. 76-88.

Monette, L.-G. (1997). *Effects of the alkali-silica reaction on unloaded, statically loaded and dynamically loaded reinforced concrete beams, PhD Dissertation.* University of Ottawa.

Morenon, P. M. (2019). Flexural performance of reinforced concrete beams damaged by Alkali-Silica Reaction. *Cement and Concrete Composites, vol. 104*, pp. 103412.

Multon, S. a. (2006). Effect of applied stresses on alkali–silica reaction-induced expansions. *Cement and Concrete Research, vol. 36, no. 5*, pp. 912-920.

Ng, K. &. (1992). Punching tests on slabs with alkali-silica reaction. *The Structural Engineer, vol. 70, no. 14*, pp. 245-252.

Nguyen, T. Y. (2019). Evaluation of elastic modulus reduction due to ASR. *Concrete in Australia, vol. 45, no. 2*, pp. 47-52.

Pan, J. F. (2012). Modeling of alkali-silica reaction in concrete: A review. *Frontiers of Structural and Civil Engineering, vol. 6, no. 1*, pp. 1-18.

Pleau, R. B. (1989). Mechanical behaviour of concrete affected by ASR. *8th International Conference on Alkali-Aggregate Reaction*, pp. 721-6.

Sanchez, L. F. (2015). Reliable quantification of AAR damage through assessment of Damage Rating Index (DRI). *Cement and Concrete Research, vol. 67*, pp. 74-92.

Sanchez, L. F. (2017). Overall assessment of Alkali-Aggregate Reaction (AAR) in concretes presenting different strengths and incorporating a wide range of reactive aggregate types and natures. *Cement and Concrete Research*, vol. 93, pp. 17-31.

Saouma, V. a. (2006). Constitutive model for alkali-aggregate reactions. *ACI Materials Journal, vol. 103, no. 3*, pp. 194-202.

Sargolzahi, M. K. (2010). Effectiveness of nondestructive testing for the evaluation of alkali–silica reaction in concrete. *Construction and Building Materials*, vol. 24, no. 8, pp. 398-403.

Smaoui, N. B. (2005). Effects of alkali addition on the mechanical properties and durability of concrete. *Cement and concrete research*, vol. 35, no. 2, pp. 203-212.

Stark, D. (1991). The moisture condition of field concrete exhibiting alkali– silica reactivity. *Proceedings of the second international conference on durability of concrete (ACI SP-126).* Montreal, Canada.

Swamy, R. N. (1992). *The alkali-silica reaction in concrete.* London: CRC Press.

Swamy, R. N.-A. (1988). Engineering properties of concrete affected by alkali-silica reaction. *ACI Materials Journal, vol. 85, no. 5*, pp. 367-374.

Takahashi Y., O. S. (2018). Nonlinear coupling models of alkali-silica reaction and multi-directional cracked reinforced concrete. *Computational Modelling of Concrete Structures – Meschke, Pichler & Rots (Eds)*, pp. 353-362.

Takahashi, Y. S. (1997). Flexural behaviour of RC beams with externally bonded carbon fiber sheet. *Proceedings of the 3rd International Symposium on on-metalic (FRP) Reinforced concrete Structures.*

Vo D., M. S. (2021). Evaluation of structures affected by Alkali-Silica reaction (ASR) using homogenized modelling of reinforced concrete. *Engineering Structures 246*, 112485.